FILM BOILING ON THE INSIDE OF VERTICAL TUBES WITH UPWARD FLOW OF THE FLUID AT LOW QUALITIES

RICHARD S. DOUGALL
WARREN M. ROHSENOW

SEPTEMBER 1963

Contract NSF G21455
Report No. 9079-26 (a)
Department of Mechanical Engineering
Massachusetts Institute of Technology

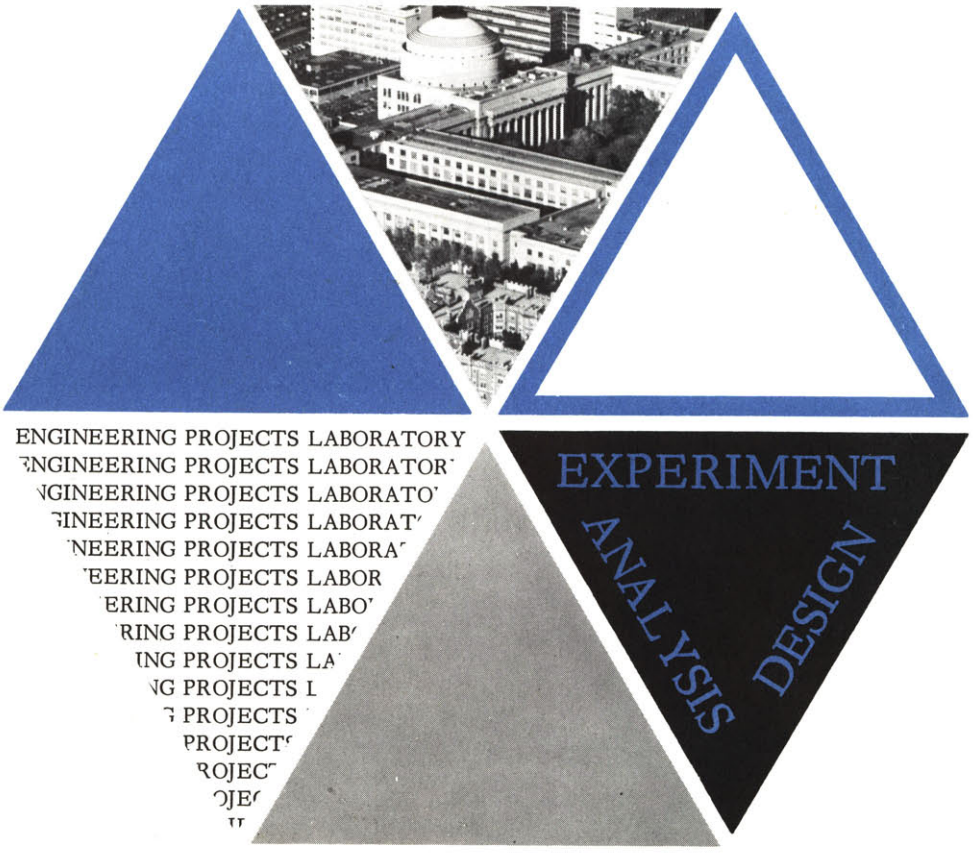

TECHNICAL REPORT NO. 9079-26

FILM BOILING ON THE INSIDE OF VERTICAL TUBES WITH UPWARD FLOW OF THE FLUID AT LOW QUALITIES

by

RICHARD S. DOUGALL
WARREN M. ROHSENOW

Sponsored by the
National Science Foundation
Contract No. NSF G-21455

Department of Mechanical Engineering
Massachusetts Institute of Technology
Cambridge 39, Massachusetts

ABSTRACT

Flow regimes, local heat transfer coefficients, and temperature distributions along the wall have been studied for film boiling inside a vertical tube with upward flow of a saturated liquid. The area of interest has been limited to cases of constant heat flux from the tube wall, small inlet liquid velocities, and film boiling which completely covers the entire heated portion of the tube. The last restriction means that there is no large region of nucleate boiling prior to the film boiling section.

A visual test section made of electrically conducting glass tubing has been used for flow visualization studies at low qualities. Visual observations with this test section have indicated that the flow regime is annular with liquid in the center and vapor along the walls of the tube. Based on interpretations of temperature distribution data, it has been concluded that the annular flow regime changes at higher qualities to one of dispersed flow--where the liquid is dispersed in the form of drops through a predominately vapor flow.

Two different diameter test sections made of stainless steel and heated electrically have been used to obtain experimental data of temperature distributions along the tube wall and local Nusselt numbers for different heat fluxes and flow rates. The fluid used in all the experimental tests has been freon 113.

For the larger tube, 0.408" I.D., heat fluxes have been varied from 14,400 to 25,600 Btu/hr-ft^2, and mass velocities have been varied from 482,000 to 818,000 lbm/hr-ft^2. For these conditions, values of heat transfer coefficients from 24.0 to 41.4 Btu/hr-ft^2-°F and values of T_w-T_s from 407 to 697°F have been obtained. These conditions have resulted in exit qualities up to 10 per cent.

For the smaller tube, 0.180" I.D., heat fluxes have been varied from 22,500 to 41,800 Btu/hr-ft^2, and mass velocities have been varied from 332,000 to 398,000 lbm/hr-ft^2. For these conditions, values of heat transfer coefficients from 27.0 to 87.5 Btu/hr-ft^2-°F and values of T_w-T_s from 261 to 883°F have been obtained. These conditions have resulted in exit qualities up to 50 per cent.

A theoretical derivation based on an annular flow model with turbulent flow in the vapor film has given good agreement with the experimental data at low qualities. A dispersed flow theory using a modified form of the Dittus and Boelter-McAdams equation seems to be an asymptote which the experimental data approaches with increasing qualities.

ACKNOWLEDGEMENTS

Financial support for this investigation was supplied by a grant from the National Science Foundation.

The authors are indebted to Professor Peter Griffith for his suggestions which led to the theory for the dispersed flow regime.

TABLE OF CONTENTS

TABLE OF FIGURES

I. INTRODUCTION

Studies of boiling liquids have led to the observation that boiling takes place in several distinct ways. This observation led to the dividing up of the boiling process into separate regimes according to the type of boiling taking place. The most common indicator of the boiling regime is the amount by which the wall temperature exceeds the saturation temperature. For moderate temperature differences, $T_w - T_{sat}$ of 10 to 100°F, the liquid touches the wall and evaporation occurs from preferred locations on the wall. This regime is called nucleate boiling. For much higher wall temperatures, $T_w - T_{sat}$ around 500°F and above, stable film boiling occurs. In stable film boiling, the liquid does not touch the walls but is kept away by a "film" of vapor completely covering the wall. Between the regimes of nucleate boiling and stable film boiling, there is a transition region where nucleate boiling occurs for part of the time and film boiling occurs for part of the time. Rohsenow (1)* or Westwater (2) has a detailed discussion of the regimes of boiling.

Nucleate boiling has been the main area for boiling research for a long time. However, film boiling is increasing in its importance because of applications in several fields of engineering. Film boiling is especially important in new applications being found for cryogenic liquids in the

* refers to Bibliography at the end of the paper

space fields.

For example, film boiling may take place in the cooling channels of regeneratively cooled rocket engines. Film boiling is also important in mono-propellant rocket systems where a fluid such as liquid hydrogen is vaporized by some device like a nuclear reactor and is then expelled through a nozzle to supply the thrust. Another important application for film boiling is in the problem of heating a fluid in a nuclear power reactor. Pressurized water reactors now are designed to operate when boiling is taking place. Since film boiling may occur locally in the reactor under some operating conditions, it becomes desirable to be able to predict the effects of film boiling on the heat transfer more exactly. These applications have led to increasing interest in theoretical and experimental investigations of film boiling.

There has been a great deal of work done on the problem of film boiling from external surfaces. Using an approximate analysis based on laminar flow in the vapor film, Bromley (3) developed a theory that gave good agreement with experimental data for film boiling from a constant temperature surface immersed in a stagnant, saturated liquid. McFadden and Grosh (4), Koh (5), and Sparrow and Cess (6) re-evaluated Bromley's theory using various types of boundary layer analyses. Sparrow and Cess included, in addition, the effect of subcooling in their analysis. Tachibana and Fukui (7) also considered subcooling, but with an integral approach. The case where the flow of vapor in a film between the stag-

nant, saturated liquid and a vertical, constant temperature wall was analyzed by Hsu and Westwater (8) using an approximate theory.

By developing a heat transfer theory based on "wave motion", Chang (9) developed an analysis for film boiling from both vertical and horizontal surfaces. Class et al (10) obtained data for film boiling from a large surface oriented vertically, at 45°, and horizontally in stagnant liquid hydrogen. By means of a stability criteria, Berenson (11) was able to obtain good agreement with experimental data for film boiling from a horizontal surface.

All the above papers considered film boiling from an external surface in a stagnant liquid. The problem of film boiling from an external surface when the liquid is moving and the flow in the film is laminar was studied by Bromley et al (12), Bradfield (13), and Sparrow and Cess (14).

In addition to film boiling from external surfaces, film boiling inside tubes has also been investigated. McDonough et al (15) obtained results for water at high pressure (2000 psig) in the transition region. They were able to operate in the transition region by controlling the wall temperature of their tube by flowing NaK over the outer wall of the tube. Polomik et al (16) also obtained experimental data for water but inside annular shaped test sections heated by passing electric current through the middle section of the annulus. The data was for the case where the water entered the test section with qualities of greater than 10 per cent.

Experimental data for cryogenic fluids inside vertical tubes has also been obtained. Lewis et al (17) obtained data for the temperature distribution after transition from nucleate to film boiling had occurred in their test section for liquid hydrogen and nitrogen as fluids. Data for film boiling of liquid hydrogen at high velocities and qualities was obtained by Hendricks et al (18). None of these papers for film boiling inside of tubes attempted to make visual observations of the two-phase regimes present during film boiling.

At the MIT Heat Transfer Laboratory, there has been a series of investigations dealing with film boiling of a liquid flowing inside a heated tube. The first study in the series was performed by Robert A. Kruger (19) who investigated film boiling heat transfer inside a horizontal tube with saturated liquid flowing in the tube. Limiting himself to the case of constant heat flux from the wall and to the case where the mass flow rate of vapor generated was small compared to the total mass flow rate, he found by visual observations that the two-phase flow regime was a stratified flow with the liquid flowing in the bottom of the tube separated from the wall by a thin vapor film and the main portion of the vapor flowing at the top of the tube above the liquid. Using this flow regime observation in his analysis, he derived a theoretical method of predicting the temperature distribution occurring over the tube's surface which agreed closely with his experimental measurements.

As a second study in this series, Edward Doyle (20)

relaxed Kruger's condition of saturated liquid flowing in the tube and considered the case of subcooled film boiling in a horizontal tube. With subcooling, the flow regime still remained of the stratified type. He found, as might be expected, that the tube wall temperatures near the inlet of the heated section were less with subcooling than those occurring for flow of saturated liquid in the tube. However, the temperatures further down the tube became hotter with subcooled liquid flow than those occurring for saturated liquid flow which was completely unexpected. He connected this phenomena to a change in the character of the vapor flow above the liquid from completely turbulent back toward laminar flow due to the subcooling and was able to bracket the experimental data between two limiting theories.

This thesis is the third study in this series. The objective is to determine the flow regime, local heat transfer coefficient, and local wall temperature for film boiling inside a vertical tube with upward flow of a saturated liquid. The investigation will be limited to cases of constant heat flux from the wall, small inlet liquid velocities and film boiling which completely covers the entire heated portion of the tube. The last restriction means that there is no large region of nucleate boiling prior to the film boiling section.

A visual test section made of electrically conducting glass tubing was used for flow visualization studies at low qualities. Visual observations with this test section indicated that the flow regime was annular with liquid in

the center and vapor along the walls.

Two quantitative test sections made of stainless steel and insulated on the outside were used to obtain experimental values of the tube wall temperature for different wall heat fluxes, flow rates, and two tube diameters. The larger tube diameter data was limited to low exit qualities and showed a nearly flat wall temperature distribution. The smaller tube diameter gave data for exit qualities up to 50 per cent. The temperature distribution for this tube diameter showed a strong decreasing trend for the higher qualities. This change in character of the temperature distribution for higher qualities was interpreted as a transition from the annular flow regime at low qualities toward a flow regime of liquid drops dispersed in a predominately vapor flow at higher qualities.

A theory has been obtained which predicts the heat transfer coefficient in the annular flow regime and indicates an asymptote toward which the dispersed flow regime tends.

II. THEORETICAL PROGRAM

A. Annular Flow Model

1. Assumptions-- The object of the theoretical program has been to find a means of predicting the local wall temperature and heat transfer coefficients for film boiling heat transfer inside a vertical tube with upward flow. The analysis is limited to film boiling where the following restrictions are satisfied. First, the heat flux from the wall is constant. Second, saturated liquid enters the heated portion of the tube. Third, film boiling covers the entire heated portion of the tube; i.e., there is no nucleate boiling section prior to the start of the film boiling section. Finally, the initial liquid velocity is not very large.

Flow visualization studies under these restrictions and at low qualities indicate that the flow regime for these low qualities is an annular flow with liquid in the center and a thin film of vapor next to the wall. (See Figs. 1 and 7.) Since the specific volume of the vapor is much larger than the specific volume of the liquid, the vapor in the film moves faster than the liquid if the film is thin and the liquid velocity is small. From the visual observations, the interface between the liquid and vapor is seen to be not smooth but variable in its thickness with substantial voids occurring in random locations. These voids maintain their identity to some degree as they travel up the tube with velocities of the order of the liquid velocity. The flow regime changes for higher qualities as will be discussed in

a later section.

The actual annular flow regime is quite complicated and it is necessary to construct a simplified mathematical model of it before it can be used. The vapor film thickness is assumed to be satisfactorily represented by its average value at any location even though random variations and oscillations of it are always present. This assumption is necessary because little is known about the actual nature of the disturbances of the liquid-vapor interface. Since the film thickness is small, the average radius of curvature of the liquid-vapor interface is of the same order of magnitude as the tube diameter. This means that the pressure can be considered uniform across tubes of normal size. Also, for the vapor Reynolds numbers corresponding to the experimental data, the flow in the film can be considered as turbulent except for a small section at the start of the film.

In order to simplify the mathematics, the following assumptions have been made.

1. Axial heat conduction is negligible both in the fluid and in the tube wall. This assumption is good for the fluid as well as for the tube wall except near the ends of the heated section.
2. All the heat can be considered to pass through the vapor film. The superheating of the vapor is then corrected for by using an effective latent heat, h'_{fg}, which includes the normal latent heat, h_{fg}, plus the heat necessary to heat the vapor to the average film temperature. Since the super-

heating is always less than the latent heat for the cases considered, this simplification should not cause too great an error in the results. (See Appendix A.)

3. The fluid properties are constant. This is not quite correct, but by an appropriate selection of the temperature at which they are evaluated, significant errors can be avoided. (See Appendix A.)
4. The film is thin enough so that the flow occurring there can be considered mathematically as flow between a plane wall and a plane liquid-vapor interface. This assumption is quite reasonable since $\frac{\delta}{D}$ is normally less than 0.1.
5. The velocity distribution in the vapor film is very similar to the universal velocity distribution in shape. This assumption will be discussed fully in the next section.
6. The momentum forces are small compared to the viscous and pressure forces. Evaluation of the theory after using this assumption shows that it is not likely to lead to significant errors.
7. Differential equations of the following form apply to the turbulent momentum and heat transport in the film.

$$\frac{\tau g_c}{\rho_{vf}} = \left(\nu_{vf} + \epsilon_m \right) \frac{dv}{dy} \qquad (1)$$

$$\frac{\left(\frac{q}{A}\right)_c}{\rho_{vf} c_{p_{vf}}} = - \left(\alpha_{vf} + \epsilon_h \right) \frac{dT}{dy} \qquad (2)$$

where y is the distance from the wall. Experience has shown these equations as quite reliable to predict turbulent flow heat transfer.

Using the above mathematical model, the governing equations will now be derived.

2. Continuity Equation--The basic equations for film boiling are derived from the equations of continuity, balance of forces, and energy. The continuity equation for the complete area of the tube is:

$$w_v + w_\ell = \text{constant} = w_T \tag{3}$$

As stated in assumption 5, the velocity distribution in the vapor film has been assumed to be similar to the universal velocity distribution in shape. This means that the velocity distribution has the following form.

$$v^+ = f(y^+, \text{roughness})$$

$$\text{where} \quad v^+ \equiv \frac{v_v}{\sqrt{\frac{\tau_w g_c}{\rho_{vf}}}} \quad , \quad y^+ \equiv \frac{y}{\nu_{vf}}\sqrt{\frac{\tau_w g_c}{\rho_{vf}}} \tag{4}$$

This type of velocity distribution can be integrated over the complete vapor film thickness giving:

$$w_v = \int_0^\delta \pi D \rho_{vf} v_v \, dy = \pi D \mu_{vf} \int_0^{\delta^+} v^+ \, dy^+ \tag{5}$$

Or, in dimensionless form,

$$\frac{4w_v}{\pi D \mu_{vf}} = 4\int_0^{\delta^+} v^+ \, dy^+ \tag{5a}$$

The quantity $\frac{4w_v}{\pi D \mu_{vf}}$ will appear quite often and will be

referred to as the vapor film Reynolds number, Re_f. The viscosity for this Reynolds number is evaluated at the film temperature, T_f.

$$Re_f \equiv \frac{4 w_v}{\pi D \mu_{vf}} \tag{6}$$

When the shape of the velocity profile is selected, the integral in equation (5a) is only a function of δ^+, and this equation relates δ^+ to the vapor film Reynolds number Re_f.

If the liquid-vapor interface was a stationary wall, the velocity distribution in the thin film would be nearly symmetrical about the middle of the film and have a shape very close to the universal velocity distribution for turbulent flow. However, the liquid-vapor interface is not a stationary wall but is moving with a finite velocity somewhat larger than the average velocity of the liquid. It would seem that the interface velocity should be closer to the average liquid velocity than the average vapor velocity because the theoretical calculations of Koh (5) and Sparrow et al (6) show that the interface velocity is nearly zero for laminar film boiling in a stagnant liquid. For theoretical conditions corresponding to those of the experimental data, the theory to be developed gives average vapor velocities of the order of 20 times larger than the average liquid velocity. Therefore, the simplest possible velocity profile to use in determining the vapor flow rate is the universal velocity distribution for turbulent flow between parallel plates.

This assumption for the velocity profile is justified because turbulent velocity distributions are relatively uniform over most of the flow area. Hence, the velocity distribution in the region near the interface contains only a small fraction of the total flow and errors in this region will have little effect when integrated to obtain the total vapor flow rate. Furthermore, roughness of the interface and interface waves complicate the actual velocity distribution to such a degree that a more refined matching of the liquid and vapor interface velocities condition does not necessarily give a better approximation for relating the film thickness and total vapor flow rate. For these reasons, the following form of the universal velocity distribution for a turbulent vapor film has been chosen.

$$\begin{aligned} 0 \leq y^+ \leq 5 \qquad & v^+ = y^+ \\ 5 \leq y^+ \leq 30 \qquad & v^+ = -3.05 + 5.0 \ln y^+ \\ 30 \leq y^+ \leq \frac{\delta^+}{2} \qquad & v^+ = 5.5 + 2.5 \ln y^+ \end{aligned} \tag{7}$$

This distribution as given above is for half the film thickness. Its mirror image is used for the other half of the film thickness.

When this velocity distribution is substituted into equation (5a) and the integration is performed, the following result is obtained.

$$\begin{aligned} &\text{For } 5 \leq \frac{\delta^+}{2} \leq 30, \quad Re_f = 100.4 - 64.4\left(\frac{\delta^+}{2}\right) + 40\left(\frac{\delta^+}{2}\right)\ln\left(\frac{\delta^+}{2}\right) \\ &\text{For } 30 \leq \frac{\delta^+}{2}, \quad Re_f = -512 + 24\left(\frac{\delta^+}{2}\right) + 20\left(\frac{\delta^+}{2}\right)\ln\left(\frac{\delta^+}{2}\right) \end{aligned} \tag{8}$$

3. Energy Equation--The energy equation written for the control volume shown in Fig. 7 is relatively simple

since the liquid is saturated and the energy that superheats the vapor can be incorporated into the latent heat. The equation is:

$$w_v h'_{fg} = \left(\frac{q}{A}\right)_T \pi D x \tag{9}$$

where x is measured from the start of the heated section. Or in dimensionless form,

$$Re_f = \frac{4\left(\frac{q}{A}\right)_T D}{h'_{fg}\,\mu_{vf}} \left(\frac{x}{D}\right) \tag{9a}$$

Equations (8) and (9a) give ways of calculating the vapor film Reynolds number and the dimensionless film thickness, $\delta^+ \equiv \frac{\delta}{\nu_{vf}} \sqrt{\frac{\tau_w g_c}{\rho_v}}$, from values of the fluid properties, heat flux, and location along the tube. However, to determine the local heat transfer coefficient or local wall temperature, values of the actual wall thickness δ or wall shear stress τ_w must be obtained. These values are obtained from force balances for the film and liquid core.

4. Force Balance--The force balance is greatly simplified by assumption 6 which states the momentum forces are negligible. Justification for this assumption is extrapolated from the theoretical investigations of laminar film boiling in a stagnant liquid. Bromley's analysis (1) was based on this assumption. Later, when mathematically more exact analyses were obtained, they were compared to Bromley's analysis and found to agree quite well with it. See references (4), (5) and (6).

The present analysis is different from the analyses

just mentioned in two important respects. First, the flow is in a tube where the liquid far from the film is no longer stationary. Second, the flow in the vapor film is turbulent instead of laminar. The first difference is not important for low quality flows because the velocity of the vapor in the film is much greater than the liquid velocity. Even with the change from laminar to turbulent flow in the film, it is expected that the relative importance of the momentum forces compared to the pressure forces and shearing forces will remain qualitatively the same.

When the theory was completed, the effect of this assumption was checked. This check showed that the momentum changes in the liquid were completely negligible for the low liquid velocities and moderate tube diameters considered. Momentum changes in the vapor film were more important than the liquid momentum, but they were still not large enough to cause changes in the film thickness or wall shear stress of more than 20 to 30 per cent. However, errors of this order will not cause similar size errors in the heat transfer coefficient which is the quantity desired, but they will usually be reduced. For these reasons, the assumption that the momentum forces are negligible was thought to be justified.

Two control volumes are used for the force balance: one for the vapor film and one for the liquid core. (See Fig. 9.) From the force balance on the two control volumes, the following equations are obtained.

$$\left(\frac{\delta}{D}\right)\frac{dp}{dx} + \frac{\tau_w}{D} + \frac{\tau_i}{D}\left(\frac{D_i}{D}\right) + \rho_v \frac{g}{g_c}\left(\frac{\delta}{D}\right) = 0 \qquad (10)$$

$$\frac{dp}{dx} - \frac{4\tau_i}{D_i} + \rho_l \frac{g}{g_c} = 0 \qquad (11)$$

Combining equations (10) and (11) gives:

$$(\rho_l - \rho_v)\frac{g}{g_c}\left(\frac{\delta}{D}\right) = \frac{\tau_w}{D} + \frac{\tau_i}{D}\left[\frac{D_i}{D} + 4\frac{D}{D_i}\left(\frac{\delta}{D}\right)\right] \qquad (12)$$

The interface shear stress should have a value somewhere between zero and the wall shear stress. Since the velocity of the vapor is so much larger than the velocity of the liquid, it is probable that the interface shear stress is nearer the value of the wall shear stress. However, as a check, both of the following cases were considered: $\tau_i = 0$ and $\tau_i[\frac{D_i}{D} + 4\frac{D}{D_i}(\frac{\delta}{D})] = \tau_w$. (The terms in the bracket are close to one for small $\frac{\delta}{D}$ and therefore were lumped into the assumption for mathematical simplicity.) For the assumption of zero shear stress at the interface and a universal velocity profile that reached its maximum at the interface, heat transfer coefficients were obtained which were significantly higher than the experimental results. However, by using the second assumption for the interface shear stress, better agreement with the experiment was obtained. (See Fig. 26 for values given by zero shear stress theory.)

Rewriting equation (12) using the assumption of equal shear stresses at the interface and wall results in:

$$(\rho_l - \rho_v)\frac{g}{g_c}\left(\frac{\delta}{D}\right) = 2\frac{\tau_w}{D} \qquad (13)$$

In dimensionless form, this equation is:

$$\left[\frac{\rho_{vf}(\rho_l - \rho_v)\, g\, D^3}{\mu_{vf}^2}\right]\left(\frac{\delta}{D}\right)^3 = 2\left(\delta^+\right)^2 \qquad (13a)$$

By the use of equations (8), (9a) and (13a), the vapor film thickness, vapor flow rate, and wall shear stress at any location along the tube can be calculated. Only two dimensionless groups need to be specified: $\frac{4\left(\frac{q}{A}\right)_T D}{h'_{fg}\mu_{vf}}$ and $\frac{\rho_v(\rho_l-\rho_v)gD^3}{\mu_{vf}^2}$. This completes the hydrodynamics of the theoretical model. The next step is to consider the heat transfer coefficient.

5. Heat Transfer Coefficient--The heat transfer coefficient desired is the one that gives the heat transferred through the film by conduction only. Once this coefficient is determined, the influence of radiation can be obtained. This heat transfer coefficient is obtained by integrating equations (1) and (2). Since the Prandtl number of most vapors is about unity, the eddy diffusivities of momentum and heat can generally be assumed to be equal. (Rohsenow and Choi (21).) This assumption is definitely good for freon 113 vapor since its Prandtl number is about 0.65.

The first step to obtain the heat transfer coefficient is to write equation (2) in integral form as follows.

$$\frac{\rho_{vf}\, c_{p_{vf}}(T_w - T)}{\left(\frac{q}{A}\right)_c}\sqrt{\frac{\tau_w g_c}{\rho_{vf}}} = Pr\int_0^{y^+}\frac{dy^+}{1 + Pr\,\frac{\varepsilon}{\nu_{vf}}} \qquad (14)$$

This equation can be integrated once the relation between ε and y^+ has been established. This relationship is obtained by combining equation (1) with the assumed velocity distribution as given in equation (7). The following assumptions first employed by Martinelli (22) and later extended for use in condensation (23) will be used.

$$\begin{aligned} &\text{For } 0 \le y^+ \le 30, && \tau \cong \tau_w \\ & && \nu_{vf} << \varepsilon \\ &\text{For } 30 < y^+, && \frac{\tau}{\tau_w} = 1 - \frac{y^+}{\delta^+/2} \end{aligned} \tag{15}$$

The assumption of a linear shear stress distribution to be used to obtain $\frac{\varepsilon}{\nu_{vf}}$ for the fully turbulent part of the film is reasonable since the momentum forces are neglected and the vapor film is assumed to be mathematically equivalent to flow between parallel planes. This particular linear shear stress distribution was chosen because it satisfies the boundary conditions of $\tau = \tau_w$ at the wall and $\tau = 0$ at the middle of the vapor film. Combining equations (1), (7) and (15), the following result is obtained for the distribution of eddy diffusivity over the vapor film.

$$\begin{aligned} &0 \le y^+ \le 5 && \frac{\varepsilon}{\nu_{vf}} = 0 \\ &5 \le y^+ \le 30 && \frac{\varepsilon}{\nu_{vf}} = \frac{y^+}{5.0} - 1 \\ &30 \le y^+ \le \frac{\delta^+}{2} && \frac{\varepsilon}{\nu_{vf}} = \left(1 - \frac{y^+}{\delta^+/2}\right)\frac{y^+}{2.5} \end{aligned} \tag{16}$$

Integrating equation (14) using the relations expressed in equation (16) is relatively straightforward from the wall out to the middle of the film, $\frac{\delta^+}{2}$. The method used to integrate equation (14) from the middle of the vapor film out to the liquid-vapor interface requires some additional discussion.

The integral in equation (14) can be looked upon as a dimensionless measure of the thermal resistance of the vapor film. The thermal resistance in the half of the vapor film next to the wall is made up of three parts: a laminar thermal resistance next to the wall, $0 \leq y^+ \leq 5$; a turbulent thermal resistance near the middle of the vapor film, $30 \leq y^+ \leq \frac{\delta^+}{2}$; and a buffer or transition thermal resistance between them, $5 \leq y^+ \leq 30$. The thermal resistance in the other half of the vapor film, next to the liquid-vapor interface will be called the "interface resistance" in the rest of this paper.

The simplest assumption for the magnitude of the interface resistance is to assume that it is equal to the resistance of the wall side. This assumption should be better for small Reynolds numbers and laminar (or close to laminar) vapor films because the resistance to heat transfer is spread fairly uniformly over the whole film thickness in this case. For higher Reynolds numbers and more turbulent vapor films, the thermal resistance per unit thickness in the laminar layer of the flow is much greater than the resistance per unit thickness in the rest of the flow. However, the liquid-vapor interface is not a plane wall but a highly mobile and oscillating surface. Therefore, it is to be expected that it is not as effective in damping out the turbulent oscillations of the vapor, and the existence of a laminar flow layer next to this surface is not very realistic. Hence, the interface resistance might be approximated as being equal in magnitude to the sum of the turbulent and buffer

thermal resistance that occur in the half of the vapor film next to the wall. As the vapor film becomes thicker, it is to be expected that even the thermal resistance which could be attributed to a buffer layer at the interface would also disappear. Then, the interface resistance would be nearly equal to the resistance of a purely turbulent flow all the way to the interface. Therefore, three expressions for the interface resistance have been considered: a LBT interface resistance theory where the interface resistance is equal to the complete resistance in the other half of the film; a BT interface resistance theory where the interface resistance is equal to the sum of the turbulent and buffer resistances in the other half of the film; and a T interface resistance theory where the interface resistance is equal to just the turbulent resistance in the other half of the film. It is now necessary to depend on experimental results to determine which of these theories to use and where it applies.

The individual thermal resistances which are used to make up the total thermal resistance of the vapor film are shown below. The expressions of equation (16) have been used in the integrals.

$$\int_0^5 \frac{dy^+}{1 + Pr\,\frac{\varepsilon}{\nu_{vf}}} = 5 \tag{17}$$

For $\frac{\delta^+}{2} < 30$

$$\int_5^{\delta_2^+} \frac{dy^+}{1 + Pr\,\frac{\varepsilon}{\nu_{vf}}} = \frac{5}{Pr} \ln\left[\frac{Pr}{5.0}\,\frac{\delta^+}{2} + (1 - Pr)\right] \tag{18}$$

For $\frac{\delta^+}{2} > 30$,

$$\int_5^{30} \frac{dy^+}{1 + Pr \frac{\varepsilon}{\nu_{vf}}} = \frac{5}{Pr} \ln (5Pr + 1) \tag{19}$$

$$\int_{30}^{\delta^+/2} \frac{dy^+}{1 + Pr \frac{\varepsilon}{\nu_{vf}}} = \frac{2.5}{Pr\sqrt{1 + \frac{10}{Pr\,\delta^+/2}}} \ln \frac{1 + \sqrt{1 + \frac{10}{Pr\,\delta^+/2}}}{1 - \sqrt{1 + \frac{10}{Pr\,\delta^+/2}}} \cdot \frac{\frac{60}{\delta^+/2} - 1 - \sqrt{1 + \frac{10}{Pr\,\delta^+/2}}}{\frac{60}{\delta^+/2} - 1 + \sqrt{1 + \frac{10}{Pr\,\delta^+/2}}} \tag{20}$$

Equation (17) is the thermal resistance of the laminar sublayer. Equation (18) is the thermal resistance of the "buffer" layer when it can be considered to extend to the middle of the vapor film. Equation (19) is the thermal resistance of the "buffer" layer when there is a turbulent region between its outer edge and the middle of the vapor film. Equation (20) is the thermal resistance of the turbulent region extending from the outer edge of the "buffer" layer to the center of the vapor film for film thicknesses greater than $\frac{\delta^+}{2} = 30$.

Using these resistances, the thermal resistances across the whole vapor film can be calculated for the three methods given above. The results of these calculations are shown in Fig. 10.

Setting $y^+ = \delta^+$ and $T = T_s$, equation (14) can be expressed in terms of a Nusselt number by the following equation.

$$Nu_f = \frac{h_c D}{k_{vf}} = \frac{\frac{\rho_{vf} D}{\mu_{vf}} \sqrt{\frac{\tau_w g_c}{\rho_{vf}}}}{\int_0^{\delta^+} \frac{dy^+}{1 + Pr \frac{\varepsilon}{\nu_{vf}}}} = \frac{\frac{\delta^+}{\delta/D}}{\int_0^{\delta^+} \frac{dy^+}{1 + Pr \frac{\varepsilon}{\nu_{vf}}}} \tag{21}$$

This equation may be presented in a more useful form by making use of equation (13a) to express $\frac{\delta^+}{\delta/D}$ in terms of the variable δ^+ alone. When this is done, the following equation is obtained.

$$Nu_f = \frac{0.794 \left[\frac{\rho_{vf}(\rho_L - \rho_{vf}) g D^3}{\mu_{vf}^2} \right]^{1/3} (\delta^+)^{1/3}}{\int_0^{\delta^+} \frac{dy^+}{1 + Pr \frac{\epsilon}{\nu_{vf}}}} \qquad (22)$$

This equation and equations (8) and (9a) enable the Nusselt number to be expressed for any vapor film Reynolds number and tube location for which the theory applies. The results for Nu_f vs. Re_f are plotted in Figs. 11, 12, and 13. These figures show how the three theories for interface resistance agree with the experimental data. The flat nature of the curves is due to the increase in heat transfer that would result from the increased flow in the film being offset by increased thermal resistance due to increases in the film thickness.

6. Local Wall Temperature--Once the local heat transfer coefficient given by equation (22) and the total heat flux from the wall are known, the corresponding local wall temperature is easily determined. It should be noted that the local heat transfer coefficient given in equation (22) is only for the heat transferred through the vapor film by conduction. Heat is also transferred by radiation from the wall directly to the liquid-vapor interface. Since the vapor film is thin, the radiation is nearly equal to that occurring between two plane surfaces. Little is known about

what emissivity to use for the liquid surface. However, since the radiation heat transfer amounts to only about 10 per cent of the total heat transferred from the wall, assumptions about this emissivity value are not very critical and a value of unity was chosen. The emissivity of stainless steel equal to 0.7 was used for the wall. The equation used to find the wall temperature then is:

$$\left(\frac{q}{A}\right)_T = h_c \left(T_w - T_s\right) + \varepsilon_{ss} \sigma \left(T_{w_{abs}}^4 - T_{s_{abs}}^4\right) \qquad (23)$$

This equation has been solved by trial and error for T_w.

B. Dispersed Flow Model

It is to be expected that the annular two-phase flow regime will not exist for all qualities. At some point along the tube, the liquid in the core and the vapor in the film will start to mix together. It is desirable to obtain an estimate of when the flow regime starts to depart from annular flow and an estimate of the magnitude of the heat transfer coefficients to be anticipated in this new flow regime.

In order to obtain these estimates, it is necessary to formulate a model for the flow regime that occurs for locations further from the start of the heated section than the annular flow regime locations. At such locations, the two phases are mixed together to some extent. The simplest model is to consider the liquid phase dispersed in the form of drops through the vapor. If there is a sufficient amount of liquid present, this liquid will help to maintain the

vapor temperature near the saturation temperature except for the vapor next to the walls of the tube.

It is to be expected that if the amount of liquid present is small, the heat transfer could be represented by a correlation for turbulent flow of pure vapor in a tube of the form:

$$Nu = 0.023\left(\frac{\rho_v V D}{\mu_v}\right)_b^{0.8} Pr_b^{0.4} \qquad (24)$$

However, since liquid is present, this correlation needs to be altered in some fashion. In film boiling, no great amount of the liquid can approach near the tube wall without being evaporated. Therefore, the liquid drops in the flow should not alter the thermal resistance of the vapor near the wall too greatly if they are not able to penetrate into this region. Since the major portion of the resistance to heat transfer occurs in the fluid next to the wall, an equation of the form shown in equation (24) should give a reasonable estimate for the heat transfer coefficient if a satisfactory value of the velocity appearing in the Reynolds number can be selected.

A velocity to choose for the Reynolds number that is easy to calculate without data concerning the distribution of the liquid in the tube and that still has physical meaning for a two-phase flow is the throughput velocity, defined as:

$$V = \frac{Q_\ell + Q_v}{A_p} \qquad (25)$$

This velocity is the total volume flow of fluid per unit

area of the pipe. It is a constant with time at any location if the inlet flow is constant, but it increases along the tube as more of the liquid is evaporated. Furthermore, when there is no longer any liquid present, this velocity reduces to the average vapor velocity needed for equation (24).

Hence, a possible correlation for the flow regime at higher qualities is:

$$Nu_s = \frac{h_c D}{k_{vs}} = 0.023 \left[\frac{\rho_{vs} D}{\mu_{vs}} \left(\frac{Q_l + Q_v}{A_p} \right) \right]^{0.8} Pr_{vs}^{0.4} \qquad (26)$$

where all the fluid properties are evaluated at the saturation temperature. The Reynolds number appearing inside the square brackets will be called the throughput Reynolds number , Re_t.

This equation may be expressed in terms of vapor film Reynolds number and film Nusselt number by the following equation.

$$\frac{h_c D}{k_{vf}} = 0.023 \frac{k_{vs}}{k_{vf}} \left[Re_f \frac{\mu_{vf}}{\mu_{vs}} \frac{h_{fg}'}{h_{fg}} \left(1 - \frac{\rho_{vs}}{\rho_l} \right) + \frac{GD}{\mu_{vs}} \frac{\rho_{vs}}{\rho_l} \right]^{0.8} Pr_{vs}^{0.4} \qquad (26a)$$

It is to be expected that this correlation should have its best accuracy for moderate qualities. At higher qualities, the results should start to deviate because there is no longer enough liquid present to maintain the bulk of the vapor at the saturation temperature. At lower qualities, the heat transfer coefficient should be higher because the liquid being in the form of larger drops will come closer

or almost touch the wall. At these lower qualities, the velocity distribution will also approach the annular flow distribution with the maximum fluid velocity occurring in the vapor near the wall. This is an additional reason for expecting the correlation in equation (26) to become less accurate. However, this correlation should provide a minimum value for the heat transfer coefficient from small qualities until qualities near unity are approached. A comparison between this correlation and the experimental data for various qualities is shown in Fig. 16.

The intersection of the dispersed flow theory with the annular flow theory provides an estimate of the vapor Reynolds number when transition occurs between the two flow regimes. This intersection is shown in Figs. 12 and 13.

C. Method of Calculation

The following approach is suggested in order to calculate the wall temperature distribution for film boiling that completely covers the inside of a vertical tube with constant heat flux from the wall and saturated liquid entering the tube at low velocities.

1. Assume a value of the vapor film temperature so that the fluid properties may be calculated at this temperature. When the analysis is completed, this assumed value can be checked and changed if this temperature would introduce significant errors. This analysis is then repeated for new values of film temperature as many times as needed until the desired accuracy is reached.

2. Evaluate the vapor film Reynolds number for various locations alone the tube by using equation (9a).

3. Determine the dimensionless vapor film thickness at these locations by using either equation (8a) or Fig. 8.

4. Determine the thermal resistance of the vapor film at these locations for the BT interface resistance theory and the T interface resistance theory by using Fig. 10.

5. Calculate the local Nusselt number at each location for both theories using equation (22). This is done by using the appropriate thermal resistances obtained in step 4 for the integral in equation (22). The BT interface resistance theory should apply for low vapor Reynolds numbers. The T interface resistance theory should apply for high Reynolds numbers. Some method is needed to determine the intermediate region. A conservative method of determining this intermediate region is to extend a horizontal line back from the minimum Nusselt number given by the T interface resistance theory until it intersects the BT interface theory and considering this line to give the Nusselt number in the intermediate region. This line is shown dotted in Fig. 12, 14 and 15.

6. Determine the Nusselt numbers given by the dispersed flow theory using equation (26a). Where these Nusselt numbers are greater than the Nusselt numbers given by the T interface resistance theory, this dispersed flow correlation should be used.

7. When the appropriate Nusselt numbers have been selected in each region along the tube, the wall temperature distribution is calculated using equation (23).

III. EXPERIMENTAL PROGRAM

The experimental program has been divided into two main objectives. One objective has been aimed at qualitatively determining the physical nature of the flow (the flow regime) present during film boiling in a vertical tube under the restrictions of constant heat flux from the wall, small inlet liquid velocities, and film boiling which completely covers the entire heated portion of the tube. The second objective has been to obtain experimental data for the wall temperature distribution and local heat transfer coefficients for this flow. In order to achieve these objectives, an apparatus was used which consisted of a visual test section, a quantitative test section, and a fluid circulation system supplying fluid to the test sections. The basic parts of the system are the same as those used by Kruger (19) and Doyle (20) in their film boiling research. Improvements were made to the basic system along with changing the orientation of the test sections from horizontal to vertical. A brief description of the various parts of the apparatus is now given. For further details, see Appendix B.

A. Description of the Apparatus

Schematic diagrams of the fluid circulation system, visual test section, and quantitative test section are shown in Figures 2, 3 and 4. Two photographic views of the apparatus are shown in Figures 5 and 6. The first photograph shows the control panel and visual test section. The second shows the fluid circulation system and the quantitative test

section.

The fluid circulation system performs those functions necessary to recirculate the fluid, freon 113, at the desired flow rate and to control the state of the fluid entering the test section. The system consists of a pump to force the fluid through the system, two preheaters to control the inlet temperature of the liquid, a condenser to condense the vapor formed in the test section, and a degasser to remove air dissolved in the freon. The degasser can also be used as a second condenser during operation. The visual and quantitative test sections are connected into the fluid circulation system in parallel so that the fluid can be bypassed through one test section while the other test section is being heated to the film boiling temperature range. A thermocouple and pressure gauge are located upstream of the test sections so the incoming state of the liquid can be determined. Additional pressure taps are located just upstream and downstream of the quantitative test section for runs with a smaller diameter tube as the test section. Finally, a thermocouple is located downstream from the condenser to insure that all the fluid leaving the condenser is liquid.

The function of the visual test section is to provide a place where film boiling may be observed in order to determine the two-phase flow regime present. It is made of a 13 mm. glass tube coated with a transparent, electrically conducting coating. A portion of the tube is heated by passing an electric current through a 9 inch length of the

coating. A variac is used to control the current supplied to the test section.

The function of the quantitative test section is to supply wall temperature data for film boiling. The test section is a 15 inch length of stainless steel tube in which the film boiling takes place due to ohmic heating in the walls of the tube. Two different diameter tubes have been used, one with a 0.408" I.D. and the other with a 0.180" I.D. Two thermocouples are located on opposite sides of the tubes at six locations along the tubes. When these tubes are installed in the apparatus, they are covered with insulation to cut down heat losses to the surroundings. In addition to the insulation, a 2.5" diameter aluminum cylinder, on which are mounted six guard heaters, is located in the insulation and placed concentrically around the test section. The power supplied to the guard heaters is controlled so that the temperature of the insulation near the guard heaters is approximately the same as the temperature of the test section. This precaution further insures that nearly all the energy generated by electrical heating in the walls of the test section is transferred to the fluid inside the test section.

Flanges are welded to the ends of the test sections. These flanges serve two useful purposes. First, they provide a means of connecting the test section with the rest of the piping. Direct metal-to-metal contact between the test section and the remainder of the piping is prevented by using gaskets between the flanges which helps somewhat to

cut down the axial conduction losses from the test section to the remainder of the piping. Secondly, the flanges are used to connect the power leads from high current capacity D.C. generators in the Heat Transfer Lab to the test section. The ohmic dissipation of the current in the tube walls supplies the heat necessary to maintain film boiling in the test section. Guard heaters are wound around the power leads near the flanges to reduce conduction losses along these leads. In order to cut down on the heat losses through the insulation, the current in the guard heaters was varied until the guard heater thermocouple read nearly the same as the corresponding pair of test section thermocouples, usually well within 100°F of each other.

A thermocouple was also mounted inside a hole drilled in each of the bus bars which connected the electric power leads to the test section flanges. The thermocouple junctions were covered with glass sleeving to prevent electrical contact with the bus bars and were tied in place. Current in the guard heaters mounted on the bus bars was controlled until the thermocouples in the bus bars read temperatures close to the temperature readings of the first and last thermocouples on the test section.

The flow rate of fluid through the test section was measured by having a calibrated rotometer in the line upstream of the preheaters where the fluid was all liquid. The accuracy was within 5 per cent for the range of values under investigation.

In addition to the temperature and flow rate measure-

ments, the heat flux from the inside wall of the test section to the fluid was obtained. Two methods were used to determine this heat flux. In the first method, the electrical power dissipated in the test section was calculated by using the measured electric current flowing through the test section and the average electrical resistivity of the test section. The relationship for the heat flux is:

$$\left(\frac{q}{A}\right)_T = \frac{1}{A_s}\left(\rho' \frac{L}{A_c}\right) I^2 \qquad (27)$$

where ρ' is the electrical resistivity of the test section determined at the average test section temperature, A_c is the cross-sectional area of the test section, L is the length of the test section, and I is the current flowing through the test section. Values of ρ' as a function of temperature for the test section material, type 304 stainless steel, were taken from reference (24).

In the second method used to determine the wall heat flux, the electrical power dissipated in the test section was calculated by using the measured electric current flowing through the test section and the measured voltage drop across the test section. For all but two runs with the 0.408" I.D. test section, the voltage pickups were located on the outside of the flanges at each end of the test section. Therefore, the power dissipation calculated using this voltage was always 7 to 15 per cent higher than the power dissipation calculated using the current and tube resistance. For this reason, it was felt that the heat flux calculated using current and tube resistance gave a more

accurate value, and this method was used in all the heat flux calculations.

The 0.408″ I.D. test section was later modified to include voltage taps welded to the tube just inside the flanges, and two runs were made with this arrangement. This arrangement was also incorporated in the construction of the 0.180″ I.D. test section and used for all the runs made with this test section. For these runs, the power dissipation in the test section as calculated by the two methods never differed by more than 7 per cent.

The current supplied to the test section was measured by measuring the voltage drop across a shunt of known resistance. Two shunts were used for this purpose. The first shunt used was one which had been calibrated at the National Bureau of Standards so that its resistance was known to within 0.1 per cent during testing conditions. The voltage across this shunt could normally be read quite accurately to four significant figures using a semi-precision potentiometer if the current was steady. However, the current supplied by the D.C. generators tended to vary randomly over a range of a few per cent of the total current output due to changes in the contact resistance of the brushes caused by slight irregularities in the commutator. These variations in the current made readings with a semi-precision potentiometer difficult because the current would not stay still long enough to balance the potentiometer. This difficulty was overcome by using a 16 channel Brown recording potentiometer and taking readings of the current

at the start and at the finish of each run. However, the absolute value of the readings given by the Bureau of Standards calibrated shunt for the currents used was a low value of the total scale reading of the recorder. Therefore, this shunt was replaced with a shunt of higher resistance which gave larger valued readings on the recorder. This second shunt was calibrated against the first shunt to give readings that were accurate within 2 per cent.

In addition to the current reading, the 16 channel Brown recording potentiometer was also wired into the system to record the test section voltage and all thermocouple readings. This recorder greatly cut down on the time required to obtain a complete set of readings since all the data could be taken with two complete passes through the 16 channels taking only 2 minutes. The thermocouples connected to the cold junction were wired directly into the recorder circuit. For the test section voltage, it was necessary to use a voltage divider to step down the magnitude of the voltage reading so that it would not exceed full scale on the recorder.

B. Instrumentation and Accuracy of Measurements

The instrumentation for the apparatus has been designed so that temperatures at various points along the test section, the flow rate of the fluid through the test section, and the heat flux from the walls of the test section may be determined.

In order to measure the temperatures, chromel-alumel

thermocouples were used. These thermocouples were tied to opposite sides of the test section at six locations: 1", $3\frac{1}{4}$", 6", 9", $11\frac{3}{4}$", and 14" from the start of the heated section. To prevent the electric current in the test section from influencing the measurements, a thin strip of mica, 0.002" thick, separated the thermocouple junctions from the tube wall. The total temperature drop between the inside of the tube and the thermocouple junction was always less than 5°F. Since the temperature difference between the inside of the tube wall and the saturation temperature of the fluid was of the order of 500°F, the temperature difference between the thermocouple junction and the inside of the wall was negligible.

In addition to the thermocouples mounted on the test section itself, other thermocouple readings were taken. Thermocouples were also located in the insulation near the guard heaters around the test section. The axial locations of these thermocouples corresponded with those mounted on the test section.

In order to evaluate the accuracy of the heat flux calculations, a heat balance was made to determine the amount of heat leaking to the surroundings and not entering the fluid. There were two main heat losses: radial conduction through the insulation and axial conduction out from the flanges to the rest of the piping and to the bus bars. The radial heat losses through the insulation were kept below 1 per cent of the total heat generated by means of the guard heaters mounted in the insulation around the test

section.

The axial conduction losses at the ends of the test section were difficult to control since the rest of the piping for the fluid must be below the saturation temperature. The bus bars, 2" x $\frac{1}{8}$" in cross section of copper originally, but later changed to nickel, were another means of conducting heat away from the ends of the test section since they were bolted directly to the outside of the flanges and were in good electrical contact with the test section. The losses through these bus bars were reduced by maintaining the temperature of the bus bars near the temperature of the test section by means of guard heaters wrapped around the bus bars. Analysis of these axial losses indicate that they were less than 5 per cent of the total heat generated. Furthermore, these losses influenced the temperature distribution only near the ends of the test section.

From this investigation of the heat losses from the test section, it seems that, with the thermocouple readings and with the heat flux determined from the electrical power dissipation in the test section, accurate values for the wall temperature distribution and the local heat transfer coefficients were obtained except for slight errors at the first and last thermocouple locations due to axial conduction. The final thermocouple readings have not been used in determining the results of the experiments. However, since the readings for the first location were generally the only readings upstream of the point of the minimum heat transfer coefficient, it eas felt that leaving this data

point out would distort the appearance of the temperature distribution. The readings for this location should not be greatly in error, but it should be remembered that they are not as accurate as the readings for the other locations used.

C. Test Procedures

With the film boiling apparatus used in this investigation, the following procedure was used to establish film boiling inside the visual test section of glass covered with a transparent electrically conducting coating. The following steps are carried out after the fluid has been degassed. The degassing operation will be discussed later in this section when the procedures for the quantitative test section are considered.

The first step is to establish the desired flow of fluid through the circulation system. Next, the hot water supplying the preheaters is adjusted to give the desired entering fluid temperature. Then, the quick-changing valves upstream from the test section are set so that the flow will bypass the glass visual test section and flow through the quantitative test section. Next, the current is turned on in the visual test section, and the entering valve is kept closed until boiling of the liquid in the test section has progressed to a state where the level of the liquid in the tube is below the heated portion of the tube. When this condition is reached, the wall temperatures in the heated portion of the tube are well above the saturation temperature of the liquid. Finally, the quick-changing valves are

reversed allowing all the liquid to flow through the visual test section, and film boiling is established in the test section. In this manner, film boiling is established without having to move continuously along the boiling curve to the peak heat flux or burnout point.

Since the glass tube was uninsulated, and heating was taking place in only a 9 inch length of the tube during the visual tests, it was impossible to maintain film boiling in the glass tube for more than 30 seconds due to axial conduction along the glass destroying the film at the start of the heated section.

With a vertical test section, the rapid motions of the disturbances on the liquid vapor interface prevent the eye from distinguishing the flow pattern in the tube. Therefore, high speed photographic techniques, which included motion pictures as well as photographs, were used to observe the flow pattern. In addition to the photography, the film boiling was observed under strobotac lighting. This presented a series of instantaneous views of the flow to the eye with the blurring effect of the motion stopped. Since the motions in the flow are random in nature and not periodic, the strobotac observations were not too clear, but they did help to interpret the photographic results.

The procedures used to obtain film boiling in the stainless steel quantitative test section are similar to those described above for the visual test section. First, the quantitative test section is bypassed by the flow while it is heated to a high temperature. The heating of the test

section during this stage of the run is accomplished mainly by means of the guard heaters although current is passed briefly through the test section at times to speed up the heating.

While the test section is heating up, the fluid is degassed to remove as much of the dissolved air in the freon 113 as possible. The degassing is accomplished by maintaining the preheaters and degassing tank as hot as possible. The degassing tank is a large tank in which the fluid velocity is quite slow so that the dissolved air can come out of solution and collect in the top of the degassing tank. The collected air is periodically bled from the tank until the gas from the tank appears to be mainly freon vapor. Then, the temperature of the fluid is regulated until it is slightly below the saturation temperature. If the flow through the visual test section is now completely liquid, the degassing is considered completed. If the flow through the visual test section is a mixture of gas and liquid, then degassing is considered to be incomplete and more vapor is bled from the degassing tank until the flow is entirely liquid.

After the degassing of the fluid and the heating up of the test section is completed, the flow rate and fluid inlet temperatures are set near the desired value for the test. Everything is now ready for film boiling of the freon 113 to be established in the test section. The next step is to pass a current through the test section of a magnitude high enough to maintain the film boiling in the tube and without

any long delay to switch the quick-changing valves allowing all the fluid to flow through the test section. It is important not to delay switching the valves very long after current is being supplied to the test section because a long delay will allow the temperatures to get dangerously high.

If the conditions are right when the fluid is started through the test section, stable film boiling is established in the test section which can be maintained in this tube indefinitely. The heat flux and flow rate are now adjusted to the proper value desired for the run. The guard heaters are controlled until the temperatures near the guard heaters approach the corresponding tube temperatures within 100°F. When this temperature balance is established, steady state operation is assumed to be attained and the data for the run is taken. The time required to reach steady state after starting with a cold system is approximately 2 hours.

When the heat flux is too low, or the freon 113 is too dirty, or the test section walls have become blackened with decomposed freon, the film boiling is not completely stable and cannot be maintained indefinitely. Under these conditions, the temperature at the start of the test section will drop until the inlet is in the nucleate boiling regime. Axial conduction along the tube wall will allow the nucleate boiling to spread until the whole test section is undergoing nucleate boiling.

From trial and error, it was found that wall temperatures 500°F above saturation and heat fluxes around 20,000 Btu/hr-ft^2-°F would usually maintain a stable film in the

test section. The flow rate of the fluid seemed to influence the transition point for a stable film to some degree. The higher the flow rate, the less stable was the film boiling. These findings are qualitatively what might be expected from a hydrodynamic viewpoint.

However, the influence of impurities is much harder to explain or predict. For example, freon obtained directly from the manufacturer and which looked colorless, tended to give more unstable film boiling than freon that had been distilled in the lab.

The blackening of the walls of the test section with decomposed freon was a more serious problem. Freon 113 decomposes to some extent at the wall temperatures occurring in the film boiling. This decomposition left a black flaky deposit on the tube walls. After several hours running in the film boiling regime, it was found that stable film boiling would not take place under identical conditions to those for which it was stable earlier in the runs. When the inside of the tube was cleaned thoroughly with alcohol, stable film boiling could be obtained again. No clear explanation for these phenomena has been found.

IV. RESULTS AND CONCLUSIONS

A. Discussion

The experimental results have shown that stable film boiling can occur inside electrically heated tubing over the entire heated portion. No attempt was made to investigate the boundary of the stable regime, where the film boiling changes to nucleate boiling, except for the qualitative results mentioned in the preceding section.

Photographs such as Fig. 1 indicate that an annular flow regime with liquid in the middle of the tube and vapor next to the tube walls occurs at positions near the inlet where the quality is low for film boiling in a vertical tube with low inlet velocities. (Kutateladze (25) has reported a similar tendency of the vapor to remain at the walls of a tube for nucleate boiling of liquids which do not wet the walls.) The liquid-vapor interface is rough with fairly large vapor voids spaced randomly along the tube wall. Motion pictures of the flow in the visual test section have established that these voids move fairly uniformly along the wall with velocities of the same order as the liquid velocity.

In the theoretical section, a mathematical description of the annular flow regime was presented. For the evaluation of the heat transfer coefficient in this flow regime, three different expressions were given to evaluate the thermal resistance of the half of the vapor film next to the liquid-vapor interface, the interface resistance. These

three expressions for the interface resistance are: a LBT interface resistance expression where the interface resistance is equal to the complete resistance existing if the liquid-vapor interface were a rigid stationary wall; a BT interface expression where the interface resistance is equal to only the sum of the turbulent and buffer resistances in the other half of the film; and a T interface resistance expression where the interface resistance is equal to just the turbulent resistance in the other half of the film.

The Nusselt numbers obtained using these expressions have been plotted against vapor film Reynolds number in Figs. 11, 12 and 13. In Fig. 11, the data for the 0.408" I.D. test section is shown for vapor film Reynolds numbers up to 10^4. The first group of data points bunched around $Re_f = 1500$, which is the data taken by the thermocouples located one inch from the start of the heated section, lies slightly above the BT interface resistance theory. These data points might be slightly high due to axial conduction out the end of the tube. The second group of data points bunched around $Re_f = 5000$, which is data for the location $3\frac{1}{4}$ inches from the start of the heated section, lies slightly below the T interface resistance theory. The final group of data points, which is for the 6 inch location, lies slightly above the T interface resistance theory. A laminar film boiling theory of Bromley's type is also shown in this figure for comparison.

In Fig. 12, the data for the 0.408" I.D. test section is shown over the complete Reynolds number range of the data

taken. The first three groupings of data points are for the locations along the tube mentioned above. The data points grouped between Re_f = 12,000 and Re_f = 25,000 are for the next two thermocouple locations, 9 inches and $11\frac{3}{4}$ inches from the start of the heated section. They again fall slightly above the T interface resistance theory. The data obtained for the last thermocouples located one inch from the end of the test section is not shown because axial conduction seems to have influenced these readings.

The T interface resistance theory seems to give fairly good agreement with the data for $Re_f > 5000$. At $Re_f = 5000$, the value of the dimensionless film thickness, δ^+, is slightly over 100. Therefore, it is reasonable to expect that the T interface resistance theory would begin to decrease in accuracy for lower vapor film Reynolds numbers since the depth of the turbulent region of the flow is no longer predominating in magnitude over the other two regions.

At these lower vapor film Reynolds numbers, the experimental Nusselt number should approach values given by the BT or LBT interface resistance theories. As it turns out, that was obtained in this region lies slightly above the BT interface resistance theory. It is not expected that the actual Nusselt numbers for very low vapor film Reynolds numbers will necessarily approach the LBT interface resistance theory because the assumption that the liquid velocity is small compared to the vapor velocity is no longer true at very low vapor film Reynolds numbers. Therefore, based on the data that was obtained, the BT interface resistance

theory should be used to calculate the Nusselt numbers near the inlet.

The exact values of Nusselt numbers in this region are not too important for their influence on the magnitude of the total heat transferred from the wall of the tube since they occur only for the first inch of the heated section. However, they are important because they can give a guide for extrapolating the theory from these low vapor film Reynolds numbers out to vapor film Reynolds numbers where the T interface resistance theory can be used with good accuracy.

A simple method of predicting Nusselt numbers for vapor film Reynolds numbers between those where the BT interface resistance theory gives good agreement with experiment and those where the T interface resistance theory gives good agreement with experiment is to extend a constant Nusselt number line back from the minimum Nusselt number given by the T interface resistance until it intersects the BT interface resistance theory. This line is shown dotted in Figs. 12, 14 and 15. If it is used as the correlation in the region between the two theories, it gives a slightly conservative method of calculating the Nusselt number.

Fig. 15 shows the effect of variations in heat flux on the Nusselt number obtained experimentally for a constant mass velocity of 8.18×10^5 lbm/hr-ft^2. Also shown on this figure are the three different annular flow theories. There seems to be no definite trend due to changes in heat flux that can be observed from the data.

Figure 14 shows the effect of variations in the liquid velocity on the Nusselt number obtained experimentally for a nearly constant heat flux. It can be seen that increasing the flow rate causes a slight increase in the Nusselt number except for the first two thermocouple locations. However, this increase in Nusselt number is not much more than 10 per cent for a flow increase of approximately 100 per cent which means that theories which ignore the influence of liquid velocity might give reasonable results.

The presentation in this paper has assumed that the interface velocity is small compared to the liquid velocity and that the interface shear stress is equal to the wall shear stress. Since the influence of liquid velocity has indeed been shown to be small by the experimental results, the theories developed previously for film boiling from external surfaces in a saturated, stagnant liquid should be compared with the present theory. The laminar theories in references (3), (4), (5) and (6) are all fairly close to the Bromley type theory shown in Figs. 11 and 26. They fall about 50 per cent below the lowest Reynolds number data and increase in error as the Reynolds number increases. Hsu and Westwater (8) have derived a film boiling theory to include the effect of turbulence in the film. Their theory essentially considers the thermal resistance to be located only in the laminar and buffer layers at the wall. This assumption is reasonable for single phase flow in pipes since only small amounts of heat are transferred near the centerline of the pipe. However, for film boiling, nearly all the heat

passes completely through the vapor film resulting in appreciable thermal resistance even in the turbulent region of the film as is shown by Fig. 8. In addition, their theory was developed for the case of constant wall temperature and neglected radiation from the walls. As is seen in Fig. 26, this theory gives values that are too high.

Before the theory presented in this paper was developed, many other possible theories were tried. One of these theories was the assumption that the liquid-vapor interface shear stress was zero. The velocity profile used for this assumption was a continuously increasing velocity profile of the universal velocity profile type where the maximum velocity occurred at the interface. The thermal resistances then included only one laminar, buffer, and the rest turbulent layer resistances. This theory gave results that were above the experimental data. Various other possible combinations of turbulent velocity profiles and thermal resistance combinations were tried, but these tended to either give too much variation with Reynolds number or values too far from the experiments. It is possible that when more information becomes known about the properties of the liquid-vapor interface in annular flow, a more precise theoretical correlation can be obtained for the annular flow regime in film boiling.

Figs. 17 through 25 show data for the wall temperature distribution along the tube for the 0.408" I.D. test section. The theory indicated on the graphs is the one based on the BT interface resistance theory for low vapor film Reynolds numbers near the inlet, the T interface resistance theory

for higher vapor film Reynolds numbers, and a transition between these two theories having a constant Nusselt number equal to the minimum value given by the T interface resistance theory. The theoretical wall temperature was calculated from the Nusselt number and heat flux by using equation (23) to correct for the radiation heat transfer from the wall. These figures show that this correlation gives a fairly accurate prediction of the maximum wall temperature. The theoretical values for the transition to dispersed flow would be at higher values of x/D than are shown on these graphs. The last experimental point is one inch from the end of the heated section and therefore probably reads a little low due to axial conduction along the tube.

Fig. 13 shows a comparison between experiment and theory for the 0.180" I.D. test section. The experiments show a somewhat higher Nusselt number near the inlet than the annular flow correlation suggested above would indicate. Farther from the inlet, the results show a substantial increase in Nusselt number with increasing vapor film Reynolds number. This strong increase in Nusselt number with Reynolds number can be explained by a change from the annular flow regime to the dispersed flow regime.

Before discussing the dispersed flow regime, some discussion of the annular flow regime in this size tube is worthwhile. This data shows a Nusselt number somewhat further above the annular flow theories than was the case for the larger tube diameter. This can partly be explained by axial conduction causing a slight error in the first thermo-

couple readings toward slightly higher Nusselt numbers. However, the main cause of the discrepancy is probably the increase in the film thickness relative to the tube diameter. For $Re_f = 5000$, $\delta/D = 0.09$. Since perturbations in the film thickness of double the average film thickness do not appear unreasonable after observing an actual vapor film as shown in Fig. 1, these larger relative perturbations for the small tube probably exert a much stronger influence on the liquid. Therefore, the assumption that the flow can be considered as occurring between a plane wall and a plane liquid-vapor interface no longer appears too reasonable.

Furthermore, because of the increase in the film thickness with respect to diameter, it is expected that the transition from annular to dispersed flow will occur sooner. The data in Fig. 13 confirms this fact. Locations along the tube with vapor film Reynolds numbers greater than 10^4 are probably in the dispersed flow regime.

The influence of mass velocity on the heat transfer coefficient obtained by using the dispersed flow theory is small since the volume flow rate of the vapor is so much larger than the volume flow of the liquid. The magnitude of this effect is shown in Fig. 12 for the two extremes of mass velocity. This effect is completely negligible for the variation of mass velocities occurring among the smaller tube data.

The experimental data, as shown in Fig. 16 where $Nu_s/Re_t^{0.8}$ is plotted against quality, shows that the dispersed flow theory improves in accuracy as the quality

increases. Furthermore, this figure shows that the transition from the annular flow regime to the dispersed flow regime occurs at qualities around 10 per cent. The value of 10 per cent quality as the transition point is approximate since the transition from one regime to the other is gradual.

The transition point can be determined analytically by assuming transition occurs at the intersection of the dispersed flow theory with the annular flow theory based on T interface resistance. From Figs. 12 and 13, it can be seen that this method of predicting transition agrees quite well with the experimental data.

Several other investigators have presented data for film boiling inside vertical tubes. The annular flow theory could not be checked with this data because annular flow as defined here was not present due to substantial amounts of nucleate boiling occurring before the film boiling section that caused the center of the flow to be a two-phase mixture throughout the film boiling region. However, the dispersed flow theory could be compared with this data.

McDonough et al (15) studied transition from partial film boiling (sometimes called transition boiling) into stable film boiling for water at 2000 psi. A typical sample of their data is shown in Fig. 27. It can be seen that their data is approaching the dispersed flow theory to some degree.

Polomik et al (16) studied film boiling of water inside an annular shaped test section at various pressures. The water entered their test section with varying amounts of

inlet quality. Their data for a pressure of 800 psi is shown in Fig. 27. Here the data seems to be more definitely approaching the dispersed flow theory.

Hendricks et al (18) studied film boiling of liquid hydrogen inside round tubes. They had various amounts of nucleate boiling in their test sections prior to the region of film boiling. Typical runs of their data are shown in Fig. 28. Here again, there seems to be a definite trend of the data toward the dispersed flow theory.

From these comparisons, it seems that the dispersed flow theory as derived here gives a conservative estimate of the film boiling heat transfer over a wide range of conditions.

B. Summary of Conclusions

The conclusions discussed in the preceding section are summarized below.

1. Stable film boiling can occur over the entire length of an electrically heated test section with upward flow of the liquid.
2. Annular flow, with liquid in the middle of the tube and vapor next to the tube wall, is the flow regime for film boiling with low inlet velocities at positions near the inlet where the quality is low.
3. In the annular flow regime, the liquid-vapor interface is rough with fairly large voids spaced randomly along the wall. These voids move fairly uniformly along the wall with velocities of the

same order as the liquid velocity.

4. Flow with liquid drops dispersed in the vapor is the flow regime in film boiling at positions farther from the inlet where the quality is high.
5. Transition between the two flow regimes seems to occur at qualities around 10 per cent for the range of test conditions studied here.
6. For film boiling of freon 113 in a 0.408" I.D. test section, the local heat transfer coefficients are nearly constant for low qualities. Their general trend along the tube is to decrease initially, reach a minimum, and start a gradual increase further down the tube. There seems to be a slight increase in the heat transfer coefficient due to an increase in the flow rate. Variations of heat flux do not seem to influence the heat transfer.
7. For film boiling of freon 113 in a 0.180" I.D. tube, the local heat transfer coefficients tend to be higher initially and increase much more rapidly with distance down the tube than those in a larger tube. The effect of changing the flow rate and heat flux again do not appear very significant.
8. For low vapor film Reynolds numbers near the start of film boiling in the annular flow regime, the BT interface resistance theory gives good agreement between experimental and theoretical Nusselt numbers.
9. For higher vapor film Reynolds numbers, the T inter-

face resistance theory gives Nusselt numbers that agree with experiments.

10. The minimum Nusselt number given by the T interface resistance theory can be considered to give a good estimate of the minimum Nusselt number occurring during film boiling in the annular flow regime. This minimum Nusselt number also gives reasonable agreement with the data in between the BT and T interface resistance theories.

11. When calculating the Nusselt numbers in the annular flow regime by the BT and T interface resistance theories, the following equation is used.

$$\frac{h_c D}{k_{vf}} = \frac{0.794\left[\frac{\rho_{vf}(\rho_l-\rho_{vf})\, g\, D^3}{\mu_{vf}^2}\right]^{1/3}(\delta^+)^{1/3}}{\int_0^{\delta^+}\frac{dy^+}{1+Pr\,\frac{\epsilon}{\nu_{vf}}}} \qquad (22)$$

The distinction between the two theories is the value used for the integral in the denominator of this expression. Values of this integral corresponding to each theory are shown in Fig. 10.

12. Expressions relating the dimensionless film thickness, δ^+, to the vapor film Reynolds number and relating the vapor film Reynolds number to tube location are:

For $5 < \frac{\delta^+}{2} < 30$,

$$Re_f = 100.4 - 64.4\left(\frac{\delta^+}{2}\right) + 40\left(\frac{\delta^+}{2}\right)\ln\left(\frac{\delta^+}{2}\right) \qquad (8)$$

For $30 < \frac{\delta^+}{2}$,

$$Re_f = -512 + 24\left(\frac{\delta^+}{2}\right) + 20\left(\frac{\delta^+}{2}\right)\ln\left(\frac{\delta^+}{2}\right) \quad (8)$$

$$Re_f = \frac{4\left(\frac{q}{A}\right)_T D}{h_{fg}' \mu_{vf}} \left(\frac{\chi}{D}\right) \quad (9a)$$

13. The heat transfer coefficient in the dispersed flow regime can be estimated by the following equation.

$$\frac{h_c D}{k_{vs}} = 0.023 \left[\frac{\rho_{vs} D}{\mu_{vs}} \left(\frac{Q_l + Q_v}{A_p}\right)\right]^{0.8} Pr_{vs}^{0.4} \quad (26)$$

This equation is applied for vapor film Reynolds numbers greater than the vapor film Reynolds number obtained by the intersection of this theory with the T interface resistance theory.

14. In calculating the wall temperatures from the theoretical Nusselt numbers, the following equation is used to correct for the radiation heat transfer through the vapor film.

$$\left(\frac{q}{A}\right)_T = h_c\left(T_w - T_s\right) + \varepsilon_{ss}\sigma\left(T_{w_{abs}}^4 - T_{s_{abs}}^4\right) \quad (23)$$

NOMENCLATURE

A_c Cross sectional area of the wall material in the test section

A_s Inside surface area of the test section

A_p Cross sectional area for fluid flow through the test section

c_p Specific heat

D Inside diameter of the test section

E Voltage drop across test section

G Mass velocity, $\frac{w_t}{A_p}$

g Gravitational acceleration

h_c Local conduction heat transfer from the walls of the test section

h_{fg} Latent heat

h'_{fg} Effective latent heat, $h'_{fg} = i_f - i_{sl}$

i_f Enthalpy of vapor at film temperature

i_{sl} Enthalpy of saturated liquid

I Electric current passing through walls of the test section

k Thermal conductivity

L Length of test section

Nu Nusselt number, $\frac{h_c D}{k_v}$

Pr Vapor Prandtl number, $\frac{c_{p_v} \mu_v}{k_v}$

p Pressure

$(\frac{q}{A})_c$ Heat transfer rate from walls of the test section by conduction

$\left(\frac{q}{A}\right)_R$ Heat transfer rate from walls of the test section by radiation

$\left(\frac{q}{A}\right)_T$ Total heat transfer rate from walls of the test section, $\left(\frac{q}{A}\right)_C + \left(\frac{q}{A}\right)_R$

Q_l Average volume flow rate of liquid at any point in the test section

Q_v Average volume flow rate of vapor at any point in the test section

Re_f Vapor film Reynolds number

Re_t Reynolds number based on through put velocity, $\frac{\rho_{vs} D}{\mu_{vs}} \left(\frac{Q_l + Q_v}{A_p}\right)$

T_f Average temperature of vapor in film next to wall, $\frac{1}{2}(T_w + T_s)$

T_s Saturation temperature

T_w Wall temperature

v Velocity of the vapor in the vapor film at various distances from the wall

v^+ Dimensionless velocity, $\frac{v}{\sqrt{\frac{\tau_w g_c}{\rho_{vf}}}}$

V_v Average velocity in the vapor film, $\frac{w_v}{\rho_v \times \text{area of vapor film}}$

V_l Average velocity in the liquid core, $\frac{w_v}{\rho_l \times \text{area of liquid core}}$

w_v Mass flow rate of vapor at any location along the test section

w_l Mass flow rate of liquid at any location along the test section

w_t Total mass flow rate, $w_v + w_l$

X Quality, $\frac{w_v}{w_t}$

x Distance from start of test section

y Distance from wall of test section

y^+ Dimensionless distance, $\frac{y}{\nu_{vf}}\sqrt{\frac{\tau_w g_c}{\rho_{vf}}}$

δ Thickness of vapor film

δ^+ Dimensionless thickness of vapor film, $\frac{\delta}{\nu_{vf}}\sqrt{\frac{\tau_w g_c}{\rho_{vf}}}$

ε_m Eddy diffusivity for momentum

ε_h Eddy diffusivity for heat

ε_{ss} Radiation emissivity for stainless steel

μ Dynamic viscosity

ν Kinematic viscosity

ρ Density

σ Stefan-Boltzmann constant, $\sigma = 0.1713 \times 10^{-8}$ Btu/ft^2-hr-R^4

τ Shear stress

τ_w Shear stress at the wall of the test section

τ_i Shear stress at the liquid-vapor interface

Subscripts

s Quantities evaluated at saturation temperature

f Quantities evaluated at film temperature

BIBLIOGRAPHY

1. Rohsenow, W. M.
   Heat Transfer--A Symposium
   University of Michigan, 1952, p. 101

2. Westwater, J. W.
   "Boiling in Liquids"
   Advances in Chemical Engineering, Academic Press, Inc., New York, 1956

3. Bromley, L. A.
   "Heat Transfer in Film Boiling"
   Chemical Engineering Progress, Vol. 46, 1950, p. 221

4. McFadden, P. W., and Grosh, R. J.
   "High-Flux Heat Transfer Studies: An Analytical Investigation of Laminar Film Boiling"
   AEC Research and Development Report, ANL-6060, 1959

5. Koh, J. C. Y.
   "Analysis of Film Boiling on Vertical Surfaces"
   ASME Paper No. 61-SA-31

6. Sparrow, E. M., and Cess, R. D.
   "The Effect of Subcooled Liquid on Laminar Film Boiling"
   ASME Paper No. 61-SA-29

7. Tachibana F., and Fukui, S.
   "Heat Transfer in Film Boiling to Subcooled Liquids"
   1961 International Heat Transfer Conference, International Developments in Heat Transfer, Part II, p. 219

8. Hsu, Y. Y., and Westwater, J. W.
   "Approximate Theory for Film Boiling on Vertical Surfaces"
   Third ASME-AIChE National Heat Transfer Conference, Storrs, Conn., August, 1959.

9. Chang, Y. P.
   "Wave Theory of Heat Transfer in Film Boiling"
   Journal of Heat Transfer, Trans. ASME, Series C, Vol. 81, 1959, p. 1

10. Class, C. R., DeHaan, J. R., Piccone, M., and Cost, R. B.
"Boiling Heat Transfer From Flat Surfaces"
Advances in Cryogenic Engineering, Vol. 5, K. D. Timmerhaus Ed., Plenum Press, Inc., New York, 1960.

11. Berenson, P. J.
"Film Boiling Heat Transfer From a Horizontal Surface"
ASME Paper No. 60-WA-147

12. Bromley, L. A., LeRoy, N. R., and Robbers, J. A.
"Heat Transfer in Forced Convection Film Boiling"
Industrial and Engineering Chemistry, Vol. 45, 1954, p. 2639

13. Bradfield, W. S.
"Plane Laminar Forced Convection Film Boiling with Subcooling"
Convair Scientific Research Laboratory, Research Note No. 35, July, 1960

14. Cess, R. D., and Sparrow, E. M.
"Film Boiling in a Forced Convection Boundary Layer Flow"
ASME Paper No. 60-WA-148

15. McDonough, J. B., Milich, W., and King, E. C.
"Partial Film Boiling with Water at 2000 psig in a Round Vertical Tube"
MSA Research Corporation, Tech. Report No. 62, October 8, 1958

16. Polomik, E. E., Levy, S., and Sawochka, S. G.
"Film Boiling of Steam-Water Mixtures in Annular Flow at 800, 1100, and 1400 Psi"
ASME Paper No. 62-WA-136

17. Lewis, J. P., Goodykoontz, J. H., and Kline, J. F.
"Boiling Heat Transfer to Liquid Hydrogen and Nitrogen in Forced Flow"
NASA TN D-1314, Sept., 1962

18. Hendricks, R. C., Graham, R. W., Hsu, Y. Y., and Friedman, R.
"Experimental Heat Transfer and Pressure Drop of Liquid Hydrogen Through a Heated Tube"
NASA TN D-765, May, 1961

19. Kruger, R. A.
"Film Boiling on the Inside of Horizontal Tubes in Forced Convection"
MIT Ph.D. Thesis, June, 1961

20. Doyle, E. F.
"Effect of Subcooling on Film Boiling in a Horizontal Tube"
S.M. Thesis, MIT, June, 1962

21. Rohsenow, W. M., and Choi, H.
Heat, Mass, and Momentum Transfer
Prentice-Hall, Inc., Englewood Cliffs, N. J., 1961

22. Martinelli, R. C., and Boelter, L. M. K.
U. of Cal. Publ., 5:2, 1942, p. 23

23. Seban, R. A.
"Remarks on Film Condensation with Turbulent Flow"
ASME Trans., February, 1954, p. 299

24. Mantell, C. L.
Engineering Materials Handbook
McGraw-Hill Book Company, Inc., New York, 1958

25. Kutateladze, S. S.
"General Information on the Process of Boiling"
Heat Transfer in Condensation and Boiling, AEC-tr-3770, 1952, p. 91

26. Bromley, L. A.
"Heat Transfer in Condensation, Part II, Effect of Heat Capacity on Condensate"
Industrial and Engineering Chemistry, Vol. 44, 1952, p. 2966

27. Kutateladze, S. S.
"Heat Transfer During Film Boiling"
Heat Transfer in Condensation and Boiling, AEC-tr-3770, 1952, p. 140

APPENDIX A

EVALUATION OF PROPERTIES

Since most fluid properties change to some degree with variations in temperature, the choice of temperature used in their evaluation can have a significant influence on theoretical calculations. For film boiling theories where all the vapor can be assumed concentrated in a thin film next to the wall, several investigators have found that the vapor transport properties and vapor density can be evaluated at the average film density without significant errors resulting. This assumption was used for the calculations of the annular flow theory in this paper.

However, these investigators have derived slightly different expressions for the effective latent heat which has been used to include the superheating of the vapor. By extending an analysis of laminar film condensation to laminar film boiling, Bromley (26) has suggested the following expression be used for the effective latent heat.

$$h_{fg}' = h_{fg}\left[1 + 0.4\,\frac{c_{pv}(T_w - T_s)}{h_{fg}}\right]^2 \qquad \text{(A-1)}$$

Sparrow and Cess (6) suggest the following expression which agrees closely with their exact boundary layer analysis of laminar film boiling.

$$h_{fg}' = h_{fg}\left[1 + 0.84\,\frac{c_{pv}(T_w - T_s)}{h_{fg}}\right] \qquad \text{(A-2)}$$

Another expression which was suggested by Kutateladze (27)

for laminar film boiling is:

$$h_{fg}' = h_{fg}\left[1 + 0.5\,\frac{c_{pv}(T_w - T_s)}{h_{fg}}\right] \qquad \text{(A-3)}$$

This expression equates the effective latent heat to the heat necessary to raise the temperature of a pound of saturated water to the mean temperature in the vapor film.

Hsu and Westwater (8) in their turbulent vapor film analysis have assumed that the vapor film is mainly at saturation temperature and therefore, have neglected superheating of the vapor. However, this assumption has been felt to be not completely justified because the calculations made of the thermal resistance of the vapor film show that there is a substantial temperature gradient even in the turbulent portion of the film.

Therefore, since the effective latent heat for turbulent films is probably somewhere between the laminar flow assumptions and assumption of negligible superheating, the expression suggested by Kutateladze was used because this has the most general physical justification and it gives the lowest effective latent heat of the three equations mentioned.

In the dispersed flow regime, the vapor is no longer concentrated in the film next to the wall but is spread over the complete tube area. The region of vapor in the center of the tube is probably near the saturation temperature if there are enough liquid drops present. The vapor near the wall is well above the saturation temperature.

Since the equation used in the dispersed flow regime

is a modification of the Dittus and Boelter-McAdams equation of single phase flow, the properties are evaluated in the same way as suggested for that equation, namely at the bulk temperature which is the saturation temperature for this case.

Since the major portion of the vapor flowing during dispersed flow is near saturation temperature, the superheating can be neglected and the standard latent heat can be used.

All properties of freon 113 used were taken from data supplied by the manufacturers. In a few cases, it was necessary to extrapolate this data to temperatures higher than those given. In these cases, linear extrapolations with temperature were made.

APPENDIX B

EXPERIMENTAL DESIGN

The major parts of the experimental apparatus are shown schematically in the following figures: Fig. 2, fluid circulation system; Fig. 3, visual test section; and Fig. 4, quantitative test section. Two photographic views of the apparatus are shown in Figs. 5 and 6. The first shows the control panel and visual test section. The second shows the fluid circulation system and the quantitative test section.

1. Fluid Circulation System

The fluid circulation system consists of the pump and motor, the rotameters, the preheaters, the pressure gage, the degasser, the condenser, the liquid reservoir, and the fluid thermocouples.

Pump and Motor--A Vanton Pump, model XB-S90 with a Buna-N "flex-i-liner" has been used in this apparatus. The pump has been driven by a 1 HP, AC motor. Coarse Control of the flow rate has been obtained by adjusting a valve in a fluid line which bypasses the pump.

Rotameters--Two Brooks Rotameters, model 8-1110 with a maximum capacity of 1.59 gpm of freon 113 and model 10-1110 with a maximum capacity of 6.0 gpm of freon 113 have been used in parallel in this system. For readings above the lower third of their scales, calibrations for these rotameters have indicated an accuracy within 5 per cent of the true flow. Fine control of the flow rate has been obtained

by throttling the valves immediately before the rotameters.

Preheaters--Two preheaters consisting of 6 inch diameter coils of 1/2 inch O.D. copper tubing submerged in a flow of hot water have been used to control the temperature of the freon entering the test sections. These preheaters have been connected in series. The total length of copper tubing in each preheater is 20 ft. The temperature of the freon 113 leaving these preheaters has been controlled by adjusting the temperature of the hot water supplied to the tanks containing the coils.

Pressure Gage--A standard 0 to 100 psi pressure gage has been used. In later runs with the smaller diameter quantitative test section, pressure taps upstream and downstream of the test section have been added. These pressure taps have been connected to mercury manometers. There has been reasonable agreement between the pressure readings made by both methods.

Degasser--A degasser has been constructed from a 4 inch diameter by 15 inch length cylindrical tank. Freon 113 has been supplied to the tank by 1/2 inch O.D. copper lines. This tank has been heated by a water jacket which enables the air dissolved in the freon to be driven out of solution in this tank. This air which then collects at the top of the tank has been bled off. Once the degassing operation has been completed, cold water has been run through the water jacket allowing the degasser to serve as another condenser.

Condenser--The main condenser has been constructed of

the same design as the preheaters. When cold water has been passed over the coil of the condenser, it has been able to condense all the freon vapor formed in the test section.

Liquid Reservoir--A 1.5 gallon capacity reservoir has been connected to the main fluid circulation loop. The total amount of liquid supplied to the system has been enough to maintain the reservoir partly filled with liquid at all times. The liquid level in this reservoir varies as the volume of the fluid in the system increases or decreases with increases or decreases of the vapor volume in the fluid.

Fluid Temperature Thermocouples--Chromel-alumel thermocouples, made from duplex, No. 28 gage wire covered with glass and enamel insulation, have been placed in the fluid flow just before the test section inlet and condenser outlet. By enclosing the thermocouple wires in small stainless steel tubes, the measurement junctions have been set as nearly as possible in the center of the fluid lines. Compression fittings with Teflon gaskets have been used to prevent leakage at the thermocouples.

2. Visual Test Section

The major component of the visual test section has been a 48 inch length of 0.418" I.D. pyrex tube coated on the outside with an electrically conducting, semi-transparent material. Copper clamps have been used to connect the electrical leads to the tube. A 9 inch length of tube located between the copper clamps has comprised the heated section.

Power has been supplied to the tube by a variable transformer connected to a 220 volt AC line. The electrical current supplied to the test section has been measured by an ammeter.

The glass tube has been connected to the 1/2 inch copper tubing of the fluid circulation system by means of nylon compression fittings. A quick changing valve has been located upstream of the quantitative test section allowing the flow to be bypassed through the quantitative test section when desired.

3. Quantitative Test Section

The quantitative test section has been constructed of a heated tube and a system for reducing the heat losses from this heated tube. Thermocouples have been used to measure the tube wall temperatures at various locations along the tube.

The material used for the heated tube has been type 304 stainless steel. Two different diameter heated tubes of 15 inches in length have been used. One has been of 0.408" I.D. and 0.500" O.D.; the other has been of 0.180" I.D. and 0.250" O.D. Flanges of type 304 stainless steel have been welded onto each end of these tubes.

These flanges have been used to connect the heated tube to inlet and outlet tubes. The flange connections have been made with 1/8 inch "Garlock" gasket material between the flanges. The inlet tube has been made 15 inches long; the outlet tube has been made 6 inches long. The material used

for these tubes has also been type 304 stainless steel.

Electric current has been supplied to the heated section through the bolts in the flanges. These bolts have been insulated and mounted in the flanges so that there is no electrical contact between the heated tube and the inlet and outlet tubes. As an additional precaution to prevent stray electric currents, the inlet and outlet tubes have been kept out of electrical contact with the rest of the fluid circulation system by using nylon compression fittings.

Pairs of chromel-alumel thermocouples have been tied to the heated tubes over thin (0.002 inch) pieces of mica. One thermocouple in each pair has been located in a straight line along one side of the tube; the other thermocouples in the pair have been located in a line on the opposite side of the tube. These pairs of thermocouples have been placed at the distances from the inlet of the tube indicated in Table I.

A 2.5 inch diameter aluminum tube which surrounds the heated tubes has been used as a frame to support six guard heaters. These guard heaters have been made from 20 feet of 28 gage nichrome heater wire. Each heater has been wrapped around the aluminum tube so that it covers approximately 2.5 inches of length. In order to prevent electrical insulation between the heater wires and the aluminum tube, the aluminum tube has been wrapped with asbestos tape and the heater wires have been inserted inside glass sleeving. The power supplied to the guard heaters has been controlled by

six small variable transformers which have been connected to a 110 volt AC line.

As an indicator for controlling the guard heaters, six thermocouples have been placed with their measuring junction just inside the aluminum guard heater tube. These thermocouples have been located axially along the guard heater tube so that one of these thermocouples corresponds in axial location to every pair of thermocouples mounted on the heated tube. To prevent electrical contact with the guard heater tube, the measuring junction of these thermocouples have been inserted inside ceramic tubing.

The volume between the heated tube and the guard heater tube has been filled with two carved pieces of Uniblock insulation. The entire test section assembly has also been surrounded by a layer of this same insulating material which reduces the capacity needed from the guard heaters.

Bus bars have been bolted on the outside of the flanges to give good electrical contact between the bolts and the power leads supplying the DC current that heats the test sections. Guard heaters identical to the guard heaters on the aluminum guard heater tube have been wrapped around these bus bars. A thermocouple has also been mounted inside a hole drilled in each of the bus bars. The thermocouple junction has been covered with glass sleeving to prevent electrical contact with the bus bar and has been tied in place.

All the thermocouples have been wired so that they may either be read individually on a standard potentiometer or

all read in sequence on a 16 channel Brown recording potentiometer.

TABLE I

THERMOCOUPLE LOCATIONS

Symbol for Location	Distance from Start of Heated Section
x_{1a}	1 in.
x_{1b}	1
x_{2a}	$3\frac{1}{4}$
x_{2b}	$3\frac{1}{4}$
x_{3a}	6
x_{3b}	6
x_{4a}	9
x_{4b}	9
x_{5a}	$11\frac{3}{4}$
x_{5b}	$11\frac{3}{4}$
x_{6a}	14
x_{6b}	14

All thermocouples designated by the subscript "a" lie on one side of the test section. All thermocouples designated by the subscript "b" lie on the opposite side of the test.

TABLE II

DATA FOR THE 0.408" I.D. TEST SECTION

Run	1	2	3
G - lbm/hr-ft^2	4.82×10^5	4.92×10^5	4.92×10^5
I - amps	286	271	271
E - volts	2.45	2.30	2.22
$(\frac{q}{A})_T$ - Btu/hr-ft^2	16,400	14,500	14,400
p - psig	7.0	6.5	6.5
T_s - °F	139	138	138
T_{liq} - °F	121	121	118

Location	T_w-T_s (°F)	h_c (Btu/hr-ft^2-°F)	T_w-T_s (°F)	h_c (Btu/hr-ft^2-°F)	T_w-T_s (°F)	h_c (Btu/hr-ft^2-°F)
x_{1a}	428	35.6	416	32.2	407	32.8
x_{1b}	445	34.0	433	30.7	420	31.6
x_{2a}	540	26.9	498	26.0	481	26.9
x_{2b}	545	26.6	503	25.6	485	26.6
x_{3a}	562	25.6	511	25.1	495	25.9
x_{3b}	565	25.4	511	25.1	497	25.8
x_{4a}	575	24.8	529	24.0	511	24.9
x_{4b}	579	24.6	529	24.0	511	24.9
x_{5a}	557	25.9	520	24.6	503	25.4
x_{5b}	561	25.6	520	24.6	503	25.4
x_{6a}	510	28.9	477	27.4	459	28.5
x_{6b}	519	28.3	485	26.8	464	28.1

TABLE II (Continued)

DATA FOR THE 0.408" I.D. TEST SECTION

Run	4	5	6
G - lbm/hr-ft^2	4.92×10^5	4.92×10^5	5.72×10^5
I - amps	286	286	316
E - volts	2.45	2.40	2.76
$(\frac{q}{A})_T$ - Btu/hr-ft^2	16,400	16,300	20,800
p - psig	6.0	6.0	8.0
T_s - °F	137	137	142
T_{liq} - °F	112	112	117

Location	T_w-T_s (°F)	h_c (Btu/hr-ft^2-°F)	T_w-T_s (°F)	h_c (Btu/hr-ft^2-°F)	T_w-T_s (°F)	h_c (Btu/hr-ft^2-°F)
x_{1a}	443	34.2	408	37.3	491	31.3
x_{1b}	456	33.1	426	35.5	505	30.2
x_{2a}	530	27.6	525	27.7	568	26.1
x_{2b}	530	27.6	530	27.4	573	25.8
x_{3a}	551	26.5	542	26.6	559	26.6
x_{3b}	551	26.5	542	26.6	559	26.6
x_{4a}	577	24.7	560	25.6	564	26.3
x_{4b}	577	24.7	564	25.3	568	26.1
x_{5a}	572	25.0	560	25.5	552	27.1
x_{5b}	572	25.0	559	25.6	555	26.9
x_{6a}	521	28.2	516	28.3	504	30.3
x_{6b}	525	27.9	521	28.0	510	29.9

TABLE II (Continued)

DATA FOR THE 0.408" I.D. TEST SECTION

Run	7	8	9
G - lbm/hr-ft^2	5.72×10^5	5.72×10^5	5.72×10^5
I - amps	301	331	331
E - volts	2.56	2.91	2.91
$(\frac{q}{A})_T$ - Btu/hr-ft^2	18,300	23,100	23,100
p - psig	8.0	9.0	9.0
T_s - °F	142	145	145
T_{liq} - °F	121	121	121

Location	T_w-T_s (°F)	h_c (Btu/hr-ft^2-°F)	T_w-T_s (°F)	h_c (Btu/hr-ft^2-°F)	T_w-T_s (°F)	h_c (Btu/hr-ft^2-°F)
x_{1a}	498	33.5	591	35.2	606	34.1
x_{1b}	512	32.4	607	34.1	624	32.9
x_{2a}	579	27.8	692	28.7	696	28.5
x_{2b}	580	27.8	691	28.7	697	28.4
x_{3a}	567	28.6	687	29.0	682	29.1
x_{3b}	567	28.6	687	29.0	684	29.2
x_{4a}	572	28.3	692	28.7	683	29.2
x_{4b}	576	28.0	697	28.4	692	28.7
x_{5a}	558	29.2	654	31.0	645	31.5
x_{5b}	558	29.2	654	31.0	649	31.3
x_{6a}	507	32.8	587	35.5	577	36.3
x_{6b}	516	32.1	591	35.2	585	35.7

TABLE II (Continued)

DATA FOR THE 0.408" I.D. TEST SECTION

Run	10	11	12
G - lbm/hr-ft^2	5.72×10^5	5.72×10^5	8.18×10^5
I - amps	316	313	313
E - volts	2.76	2.71	2.71
$(\frac{q}{A})_T$ - Btu/hr-ft^2	20,800	20,300	20,300
p - psig	8.0	7.5	8.0
T_s - °F	142	141	142
T_{liq} - °F	117	117	117

Location	T_w-T_s (°F)	h_c (Btu/hr-ft^2-°F)	T_w-T_s (°F)	h_c (Btu/hr-ft^2-°F)	T_w-T_s (°F)	h_c (Btu/hr-ft^2-°F)
x_{1a}	571	32.7	567	32.2	531	34.8
x_{1b}	589	31.4	581	31.2	549	33.4
x_{2a}	661	27.4	658	26.5	651	26.9
x_{2b}	666	26.8	662	26.3	653	26.8
x_{3a}	649	27.8	645	27.2	623	28.5
x_{3b}	652	27.6	649	27.0	626	28.3
x_{4a}	653	27.5	655	26.7	627	28.3
x_{4b}	660	27.1	659	26.5	631	28.0
x_{5a}	627	29.1	628	28.2	606	29.5
x_{5b}	631	28.8	633	27.9	610	29.3
x_{6a}	567	33.0	574	31.7	559	32.7
x_{6b}	576	32.4	581	31.2	566	32.2

TABLE II (Continued)

DATA FOR THE 0.408" I.D. TEST SECTION

Run	13	14	15
G - lbm/hr-ft^2	8.18×10^5	8.18×10^5	8.18×10^5
I - amps	313	298	295
E - volts	2.71	2.51	2.51
$(\frac{q}{A})_T$ - Btu/hr-ft^2	20,200	17,900	17,400
p - psig	9.0	8.5	8.5
T_s - °F	145	143	143
T_{liq} - °F	121	120	120

Location	T_w-T_s (°F)	h_c (Btu/hr-ft^2-°F)	T_w-T_s (°F)	h_c (Btu/hr-ft^2-°F)	T_w-T_s (°F)	h_c (Btu/hr-ft^2-°F)
x_{1a}	528	34.8	480	34.2	459	34.9
x_{1b}	543	33.7	489	33.4	472	33.8
x_{2a}	641	27.3	584	26.8	567	27.0
x_{2b}	645	27.0	588	26.6	579	26.3
x_{3a}	615	28.8	558	28.5	545	28.4
x_{3b}	615	28.8	558	28.5	546	28.3
x_{4a}	615	28.8	558	28.5	546	28.3
x_{4b}	611	29.0	562	28.2	546	28.3
x_{5a}	590	30.4	531	30.1	519	30.2
x_{5b}	599	29.8	535	30.0	525	29.8
x_{6a}	547	33.4	493	33.1	483	32.9
x_{6b}	556	32.7	498	32.7	486	32.7

TABLE II (Continued)

DATA FOR THE 0.408" I.D. TEST SECTION

Run	16	17	18
G - lbm/hr-ft^2	8.18×10^5	8.18×10^5	8.18×10^5
I - amps	328	325	310
E - volts	2.86	2.86	2.81
$(\frac{q}{A})_T$ - Btu/hr-ft^2	25,600	22,100	19,600
p - psig	9.0	9.0	9.0
T_s - °F	145	145	145
T_{liq} - °F	115	115	116

Location	T_w-T_s (°F)	h_c (Btu/hr-ft^2-°F)	T_w-T_s (°F)	h_c (Btu/hr-ft^2-°F)	T_w-T_s (°F)	h_c (Btu/hr-ft^2-°F)
x_{1a}	567	41.4	573	34.8	569	30.7
x_{1b}	582	40.2	586	33.9	581	29.9
x_{2a}	695	32.1	683	27.8	605	28.4
x_{2b}	696	32.0	691	27.4	633	26.8
x_{3a}	668	33.9	658	29.2	575	30.3
x_{3b}	667	33.9	658	29.2	575	30.3
x_{4a}	670	33.7	658	29.2	581	29.9
x_{4b}	670	33.7	658	29.2	567	30.9
x_{5a}	624	36.9	608	32.4	562	31.2
x_{5b}	632	36.3	614	32.0	581	29.9
x_{6a}	590	39.5	574	34.6	535	33.2
x_{6b}	594	39.2	580	34.3	496	36.3

TABLE II (Continued)

DATA FOR THE 0.408" I.D. TEST SECTION

Run	19	20	21
G - lbm/hr-ft^2	8.18×10^5	8.18×10^5	6.15×10^5
I - amps	297	328	292
E - volts	2.68	3.16	2.15
$(\frac{q}{A})_T$ - Btu/hr-ft^2	17,600	22,800	16,900
p - psig	8.5	5.0	7.0
T_s - °F	143	134	139
T_{liq} - °F	122	102	121

Location	T_w-T_s (°F)	h_c (Btu/hr-ft^2-°F)	T_w-T_s (°F)	h_c (Btu/hr-ft^2-°F)	T_w-T_s (°F)	h_c (Btu/hr-ft^2-°F)
x_{1a}	521	30.4	610	33.5	515	29.5
x_{1b}	526	30.1	622	32.7	519	29.3
x_{2a}	549	28.5	696	28.2	544	27.6
x_{2b}	566	27.4	694	28.3	540	27.8
x_{3a}	523	30.3	690	28.5	527	28.7
x_{3b}	521	30.4	673	29.5	519	29.3
x_{4a}	530	29.8	696	28.2	527	28.7
x_{4b}	530	29.8	686	28.8	523	29.0
x_{5a}	511	31.1	684	28.9	510	30.5
x_{5b}	508	31.4	669	29.7	510	30.5
x_{6a}	494	32.4	669	29.7	458	34.0
x_{6b}	480	33.6	669	29.7	441	35.5

TABLE II (Continued)

DATA FOR THE 0.408" I.D. TEST SECTION

Run	22
G - lbm/hr-ft^2	6.15×10^5
I - amps	313
E - volts	2.32
$(\frac{q}{A})_T$ - Btu/hr-ft^2	19,900
p - psig	7.0
T_s - °F	139
T_{liq} - °F	120

Location	$T_w - T_s$ (°F)	h_c (Btu/hr-ft^2-°F)
x_{1a}	570	31.3
x_{1b}	579	30.6
x_{2a}	600	29.3
x_{2b}	596	29.5
x_{3a}	579	30.6
x_{3b}	575	30.9
x_{4a}	579	30.6
x_{4b}	575	30.9
x_{5a}	557	32.2
x_{5b}	553	32.4
x_{6a}	497	36.9
x_{6b}	480	38.4

TABLE III

DATA FOR THE 0.180" I.D. TEST SECTION

Run	23	24	25
G - lbm/hr-ft^2	3.98×10^5	3.84×10^5	3.32×10^5
I - amps	161	163	174
E - volts	3.87	3.87	4.29
$(\frac{q}{A})_T$ - Btu/hr-ft^2	34,300	35,400	41,800
p - psig	2.76	2.74	2.83
Δp - psig	2.42	2.38	2.48
T_s - °F	127	127	127
T_{liq} - °F	122	122	120

Location	T_w-T_s (°F)	h_c (Btu/hr-ft^2-°F)	T_w-T_s (°F)	h_c (Btu/hr-ft^2-°F)	T_w-T_s (°F)	h_c (Btu/hr-ft^2-°F)
x_{1a}	751	40.7	777	40.4	871	41.9
x_{1b}	740	41.5	765	41.2	861	42.6
x_{2a}	769	39.5	786	39.8	883	41.2
x_{2b}	761	40.1	782	40.1	879	41.4
x_{3a}	625	51.0	629	52.3	735	51.9
x_{3b}	621	51.4	629	52.3	735	51.9
x_{4a}	565	57.2	574	58.1	684	56.7
x_{4b}	565	57.2	574	58.1	684	56.7
x_{5a}	535	60.8	540	62.2	649	60.3
x_{5b}	535	60.8	540	62.2	647	60.5
x_{6a}	535	60.8	447	76.4	556	71.8
x_{6b}	470	70.1	470	72.4	531	75.5

TABLE III (Continued)

DATA FOR THE 0.180" I.D. TEST SECTION

Run	26		27	
G - lbm/hr-ft^2-F	3.84×10^5		3.91×10^5	
I - amps	134		134	
E - volts	3.12		3.07	
$(\frac{q}{A})_T$ - Btu/hr-ft^2	23,000		22,500	
p - psig	2.08		2.04	
Δp - psig	1.90		1.81	
T_s - °F	125		125	
T_{liq} - °F	120		120	
Location	$T_w - T_s$ (°F)	h_c (Btu/hr-ft^2-°F)	$T_w - T_s$ (°F)	h_c (Btu/hr-ft^2-°F)
x_{1a}	653	31.1	563	36.5
x_{1b}	647	31.5	558	36.9
x_{2a}	725	27.0	606	33.4
x_{2b}	720	27.3	606	33.4
x_{3a}	601	34.5	524	39.7
x_{3b}	601	34.5	524	39.7
x_{4a}	504	42.6	472	44.8
x_{4b}	503	42.7	472	44.8
x_{5a}	455	47.8	442	48.2
x_{5b}	455	47.8	442	48.2
x_{6a}	261	86.3	252	87.5
x_{6b}	292	76.8	283	77.6

Figure 1. Photograph of Film Boiling Inside a Vertical Tube with G=6. 60 x 10^5 lbm/hr-ft^2

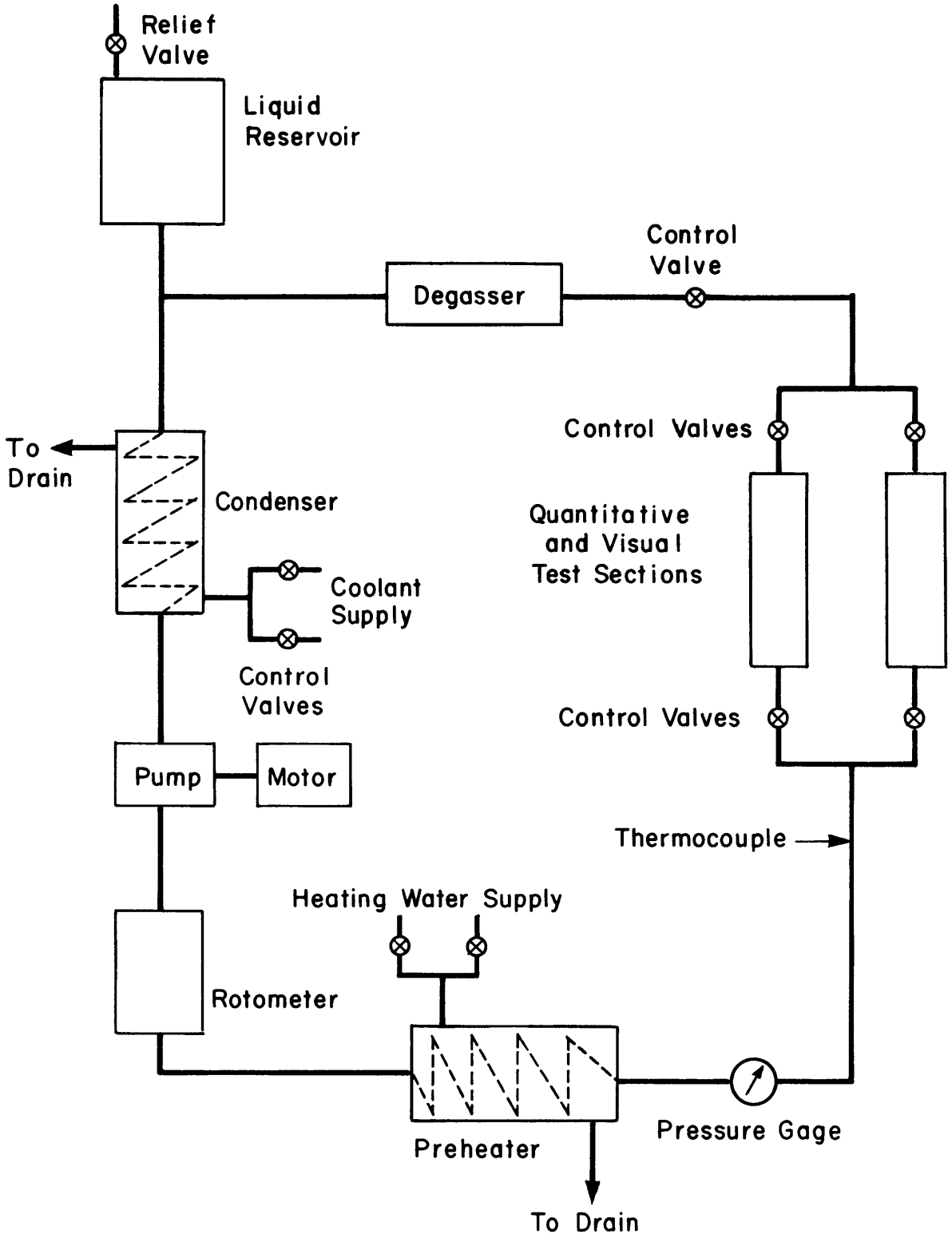

FIG. 2 SCHEMATIC DIAGRAM OF THE FREON 113 CIRCULATION SYSTEM

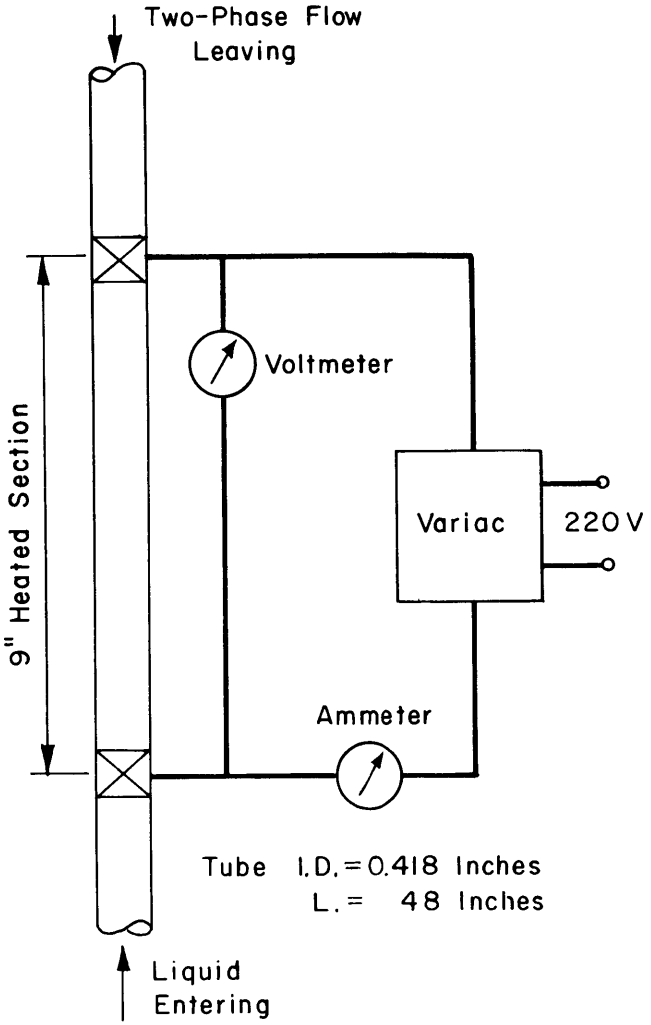

FIG. 3 SCHEMATIC DIAGRAM OF THE VISUAL TEST SECTION

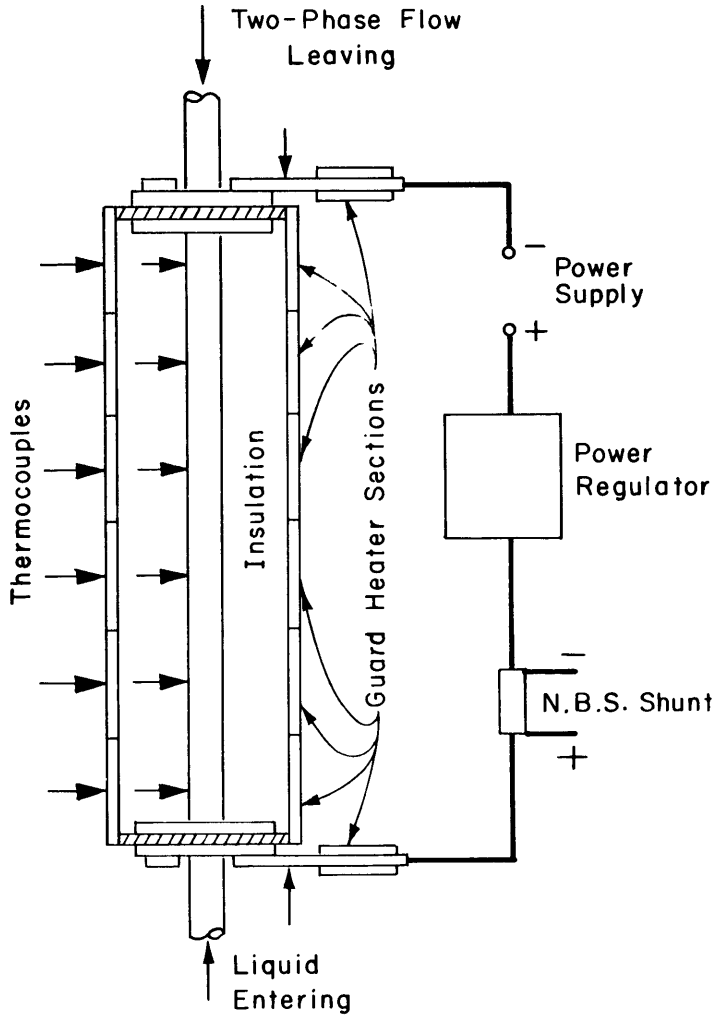

FIG. 4 SCHEMATIC DIAGRAM OF THE QUANTITATIVE TEST SECTION

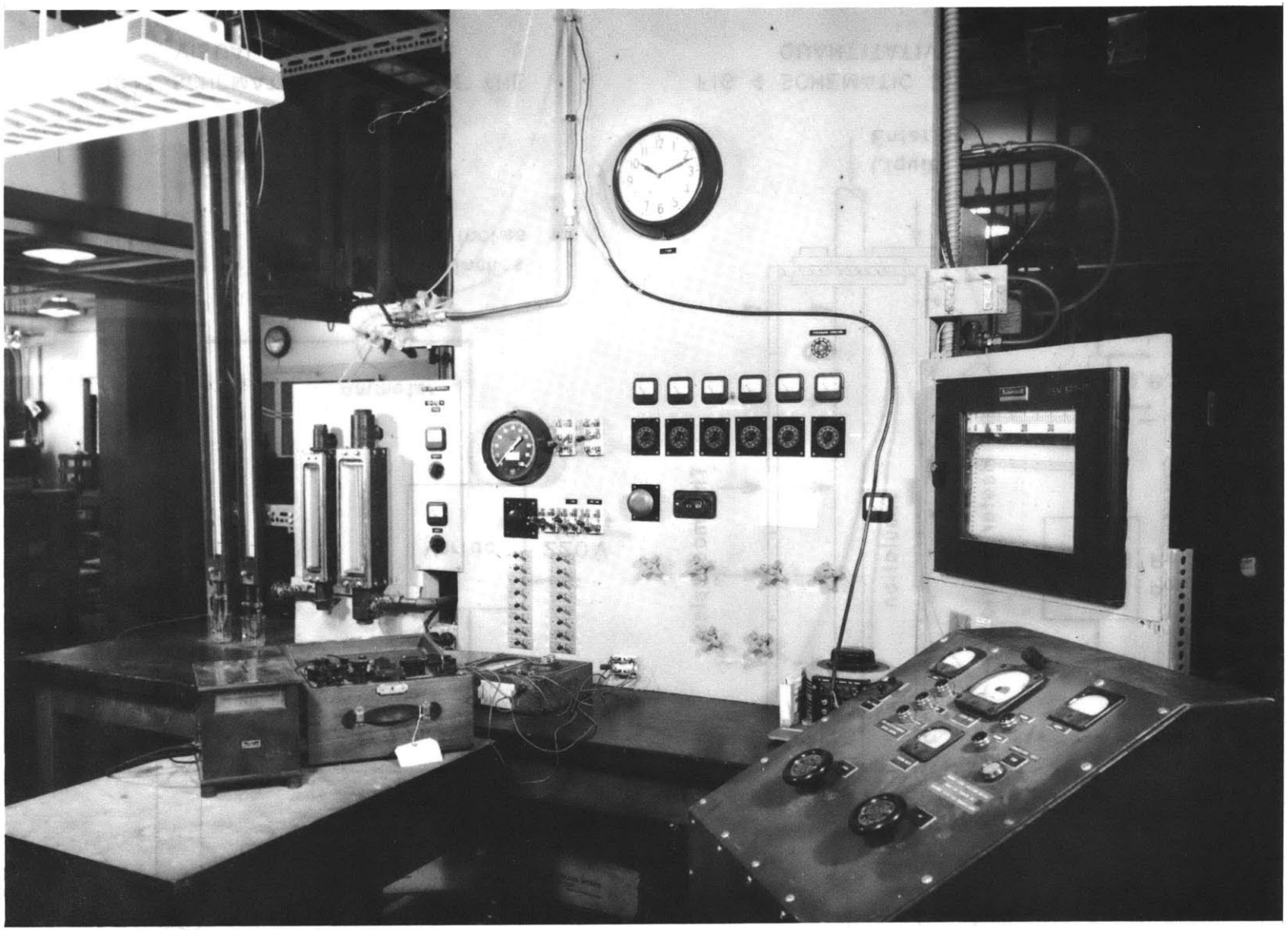

Figure 5. Photograph of the Visual Test Section and Apparatus Control Panel

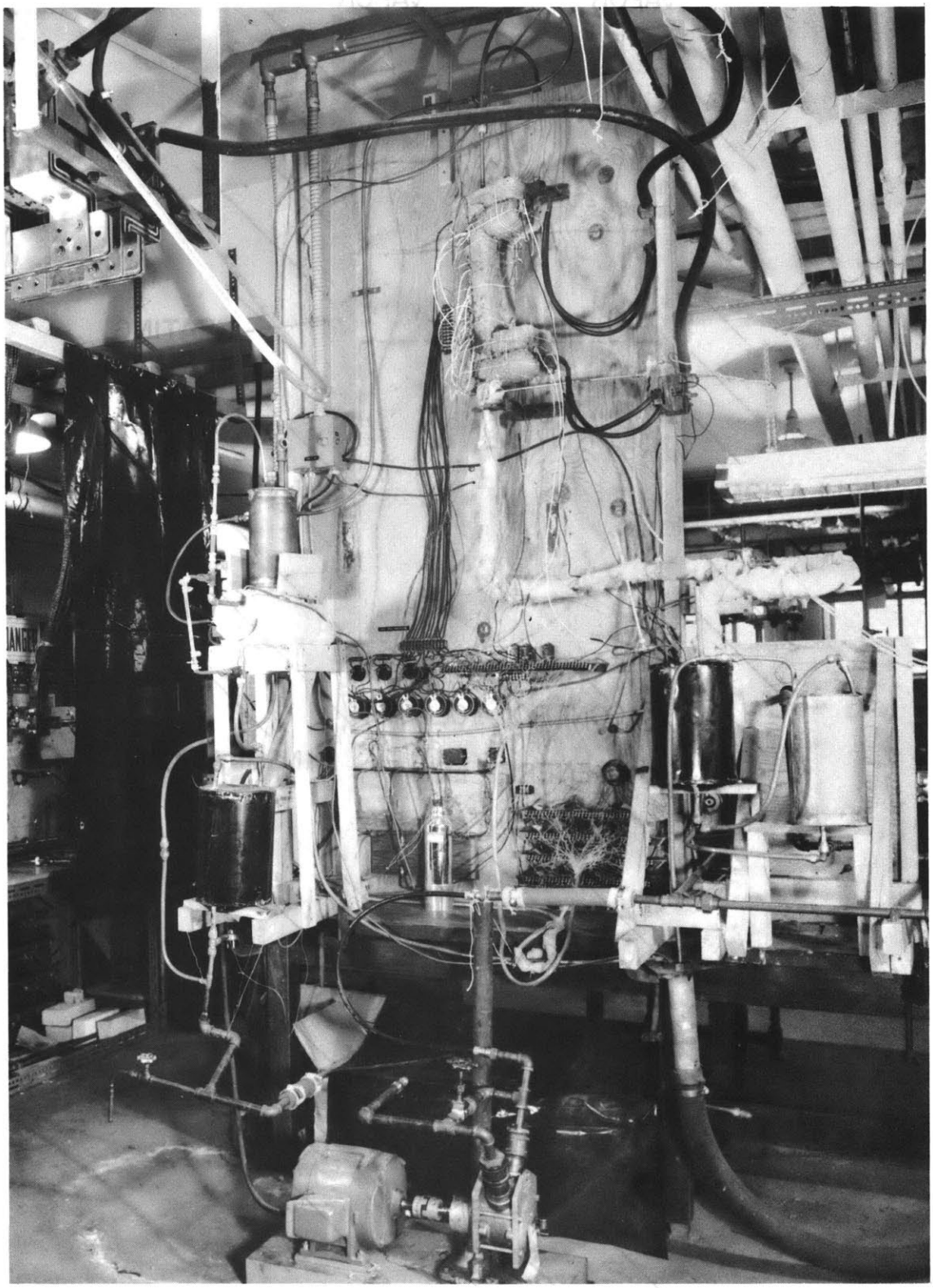

Figure 6. Photograph of the Quantitative Test Section and Fluid Circulation System

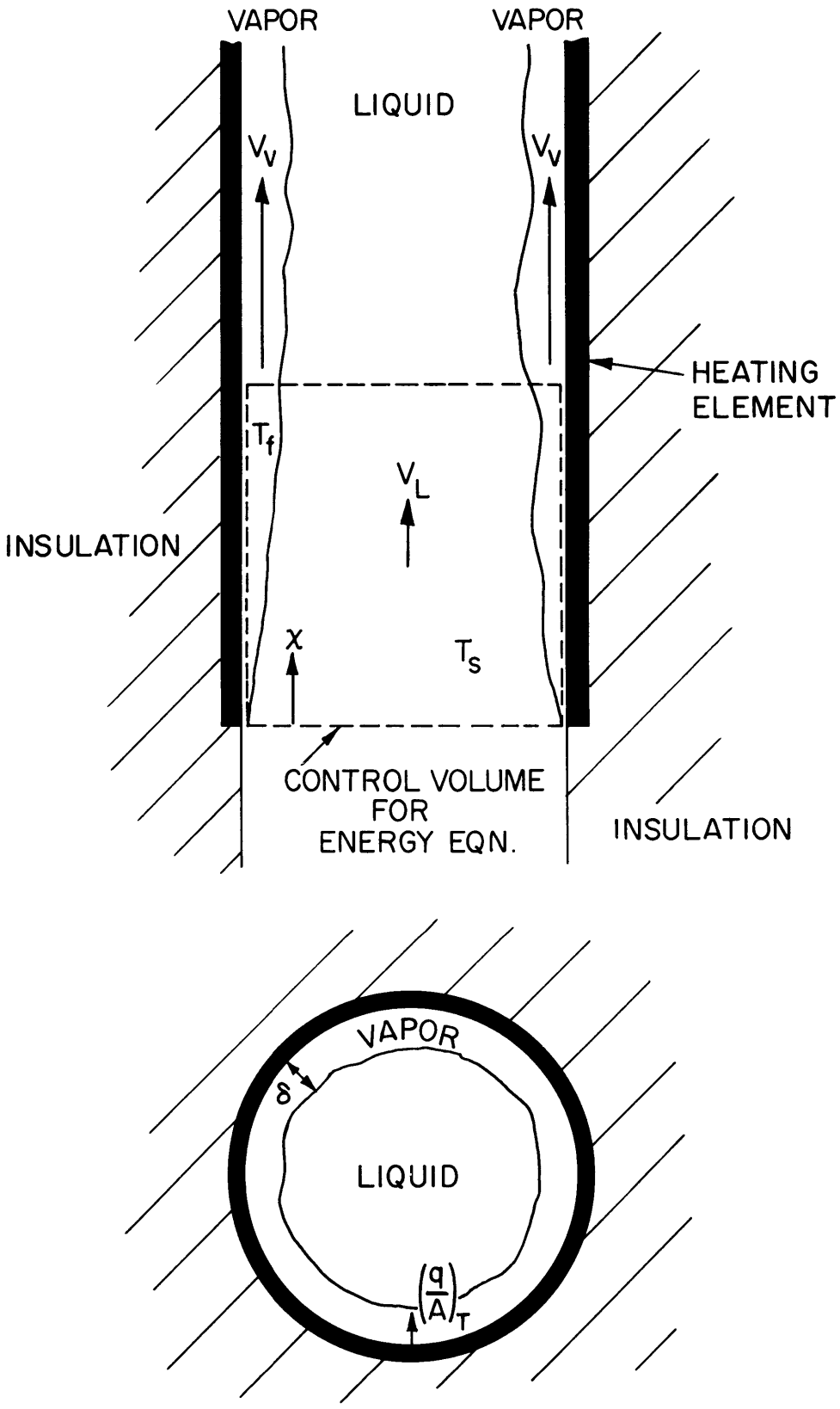

FIG. 7 IDEALIZED MODEL FOR ANNULAR FLOW REGIME

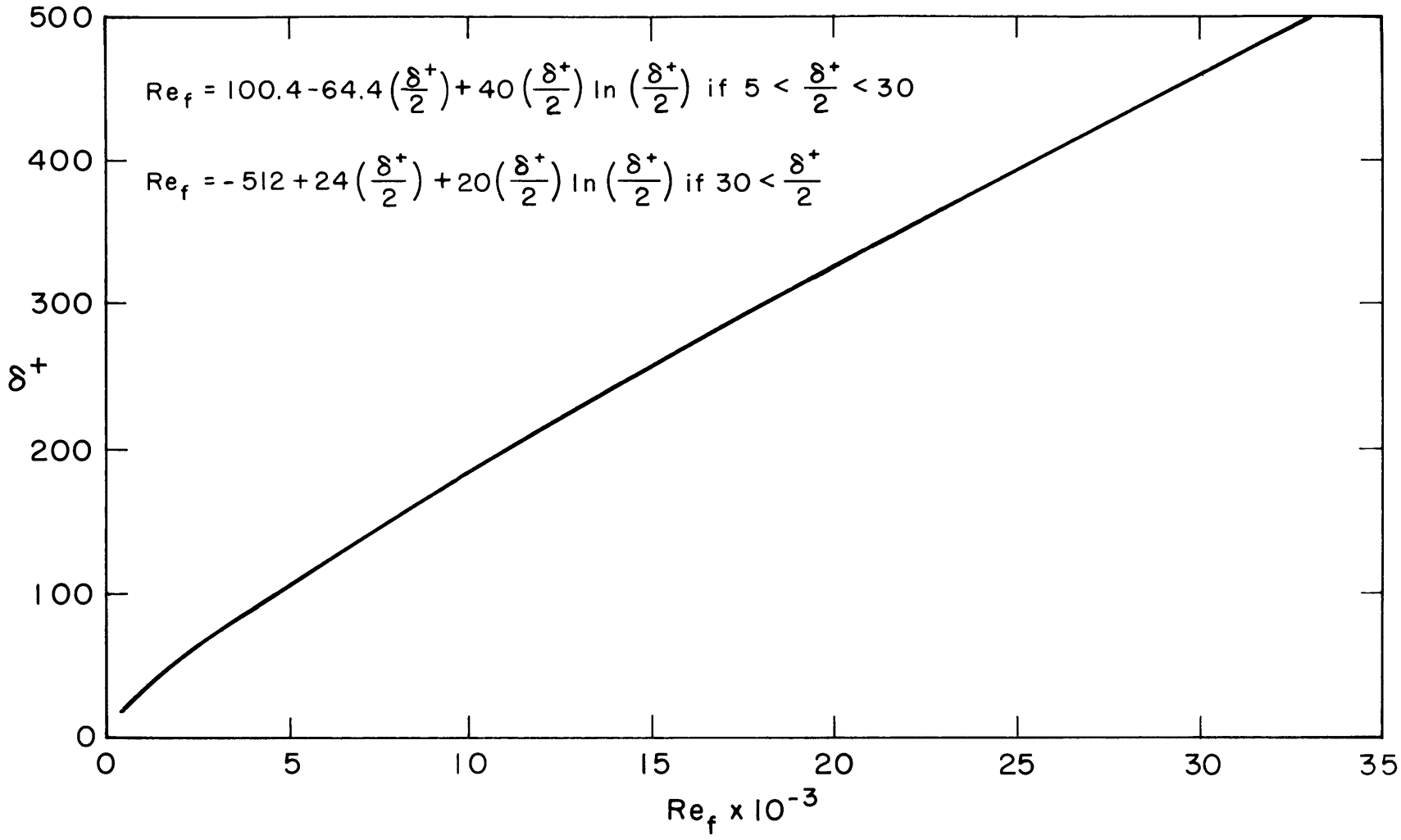

FIG. 8 RELATION BETWEEN DIMENSIONLESS FILM THICKNESS AND VAPOR FILM REYNOLDS NUMBER

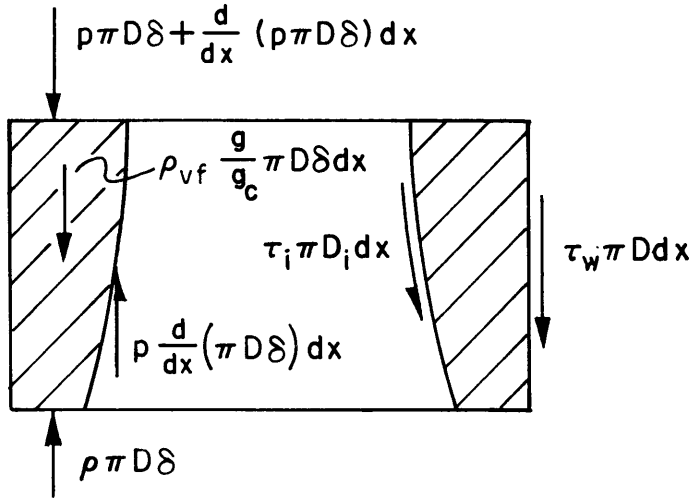

Vapor Control Volume

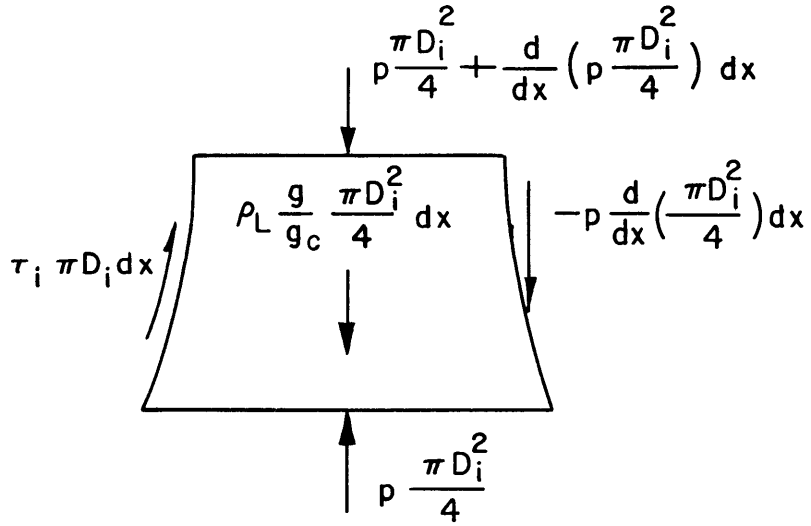

Liquid Control Volume

FIG. 9 CONTROL VOLUMES FOR FORCE BALANCE

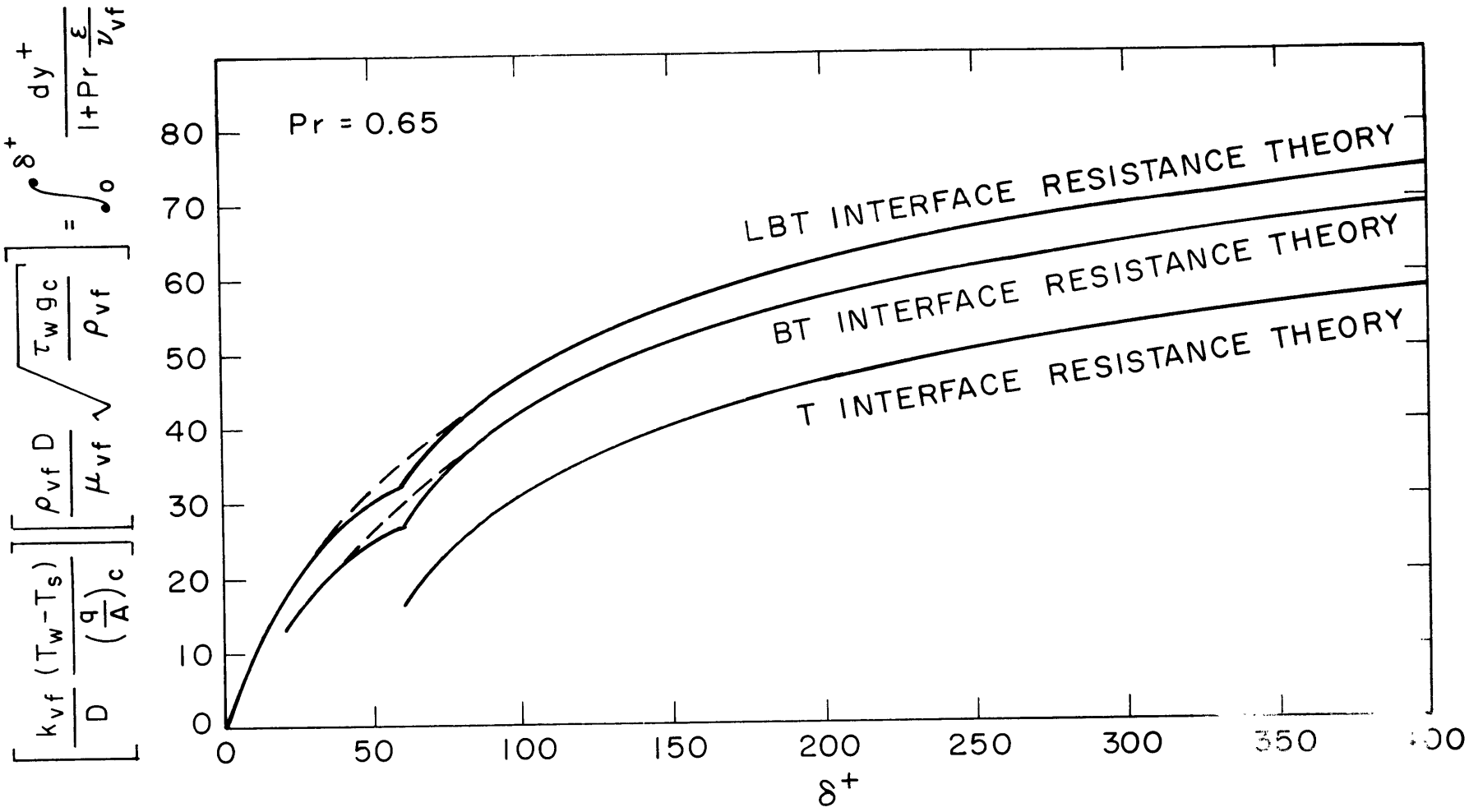

FIG. 10 THEORETICAL EXPRESSIONS FOR THE THERMAL RESISTANCE OF THE VAPOR FILM

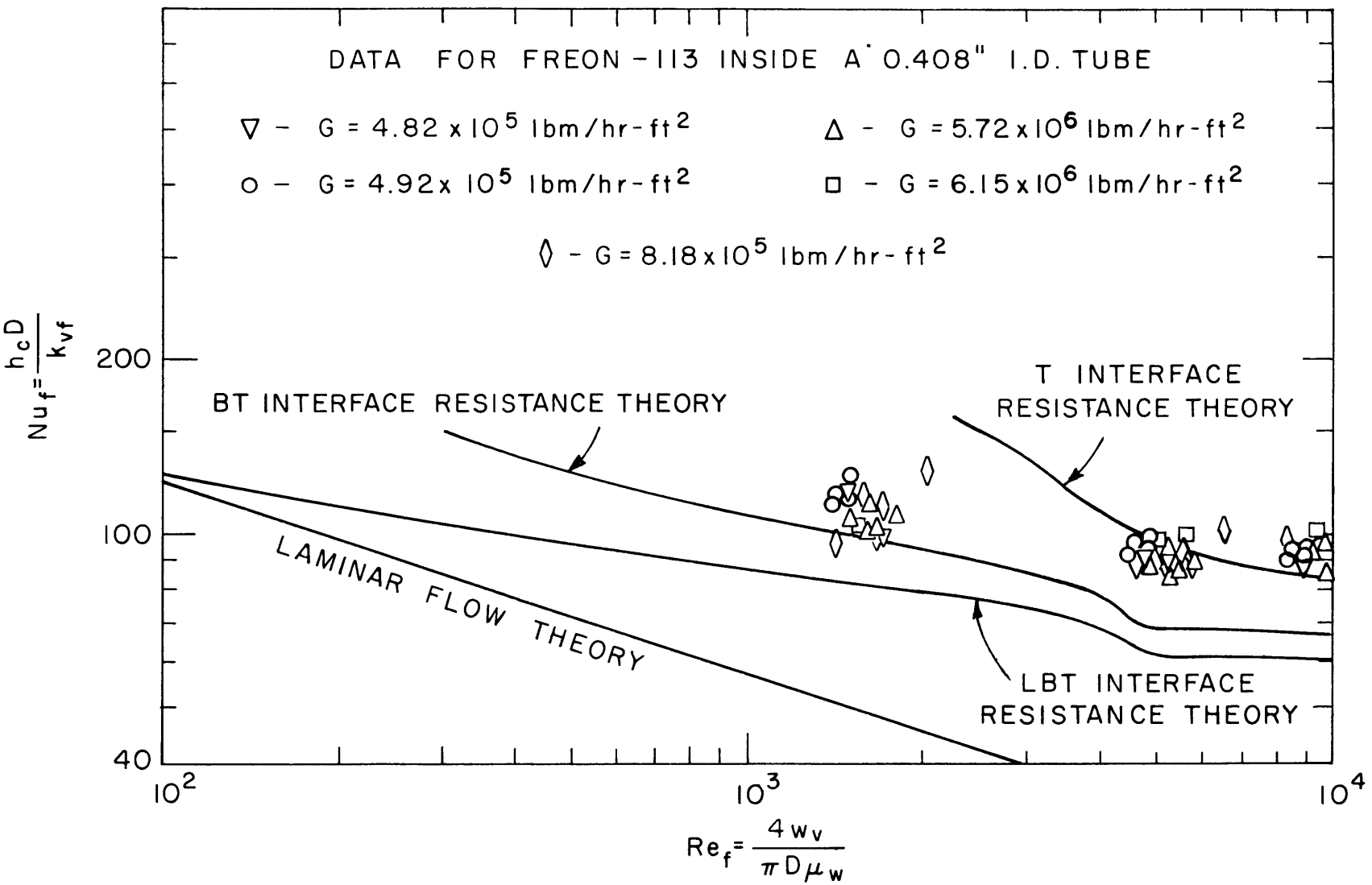

FIG. 11 COMPARISONS BETWEEN EXPERIMENT AND THEORY BASED ON ANNULAR FLOW MODEL FOR LOW REYNOLDS NUMBER RANGE

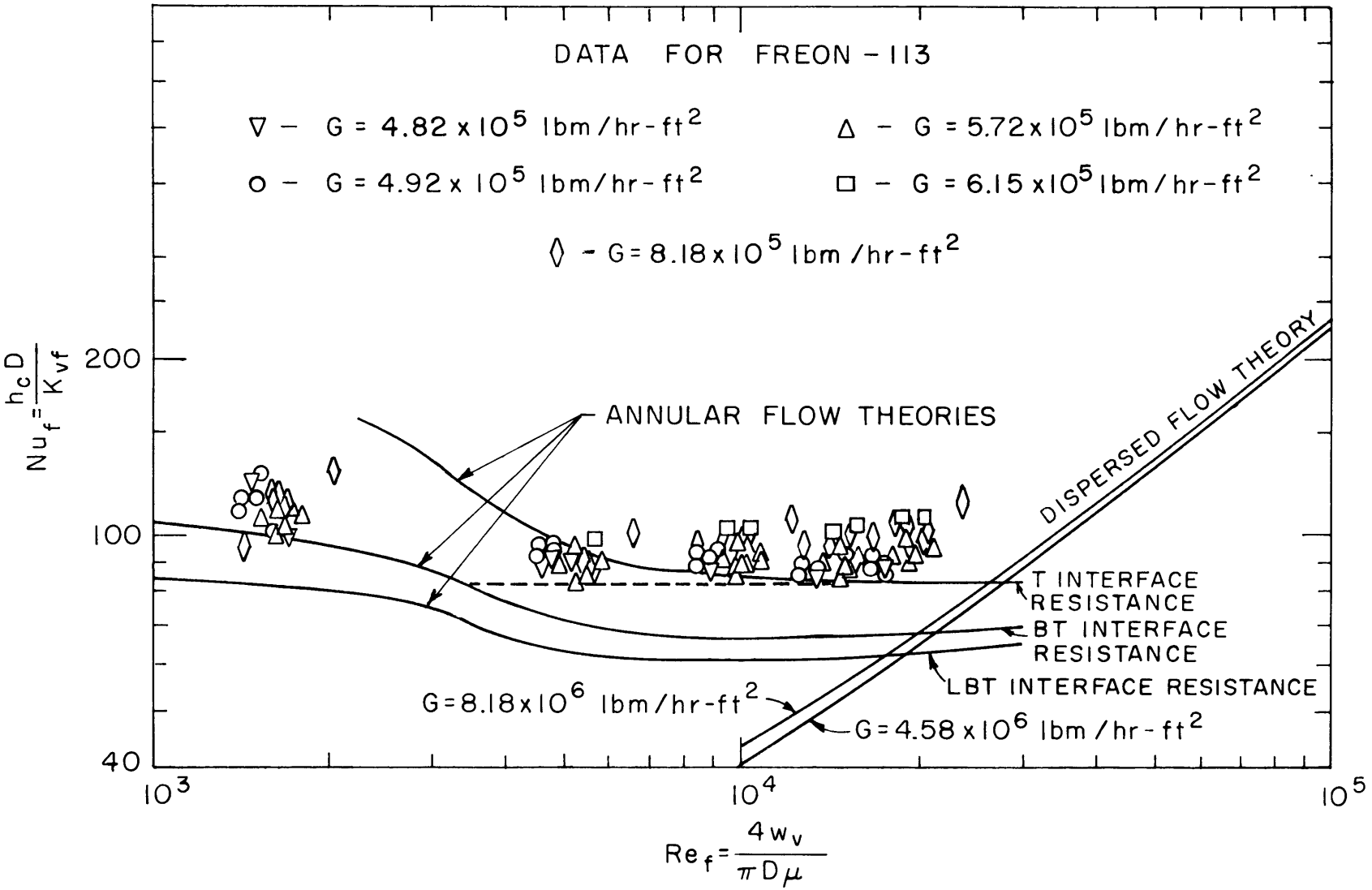

FIG. 12 COMPARISONS BETWEEN EXPERIMENT AND THEORY FOR 0.408" I.D. TUBE

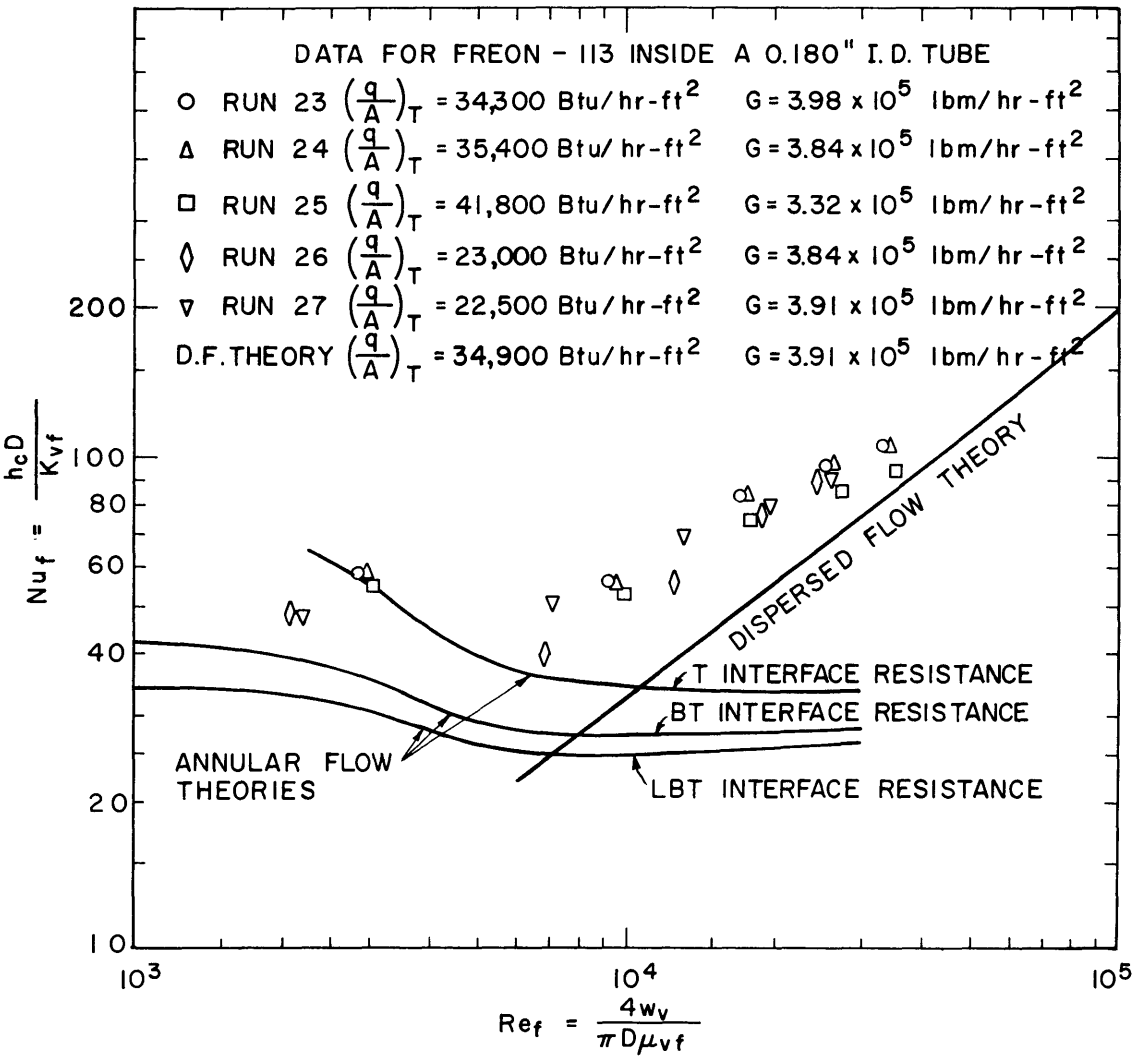

FIG. 13 COMPARISONS BETWEEN EXPERIMENT AND THEORY FOR 0.180" I.D. TUBE

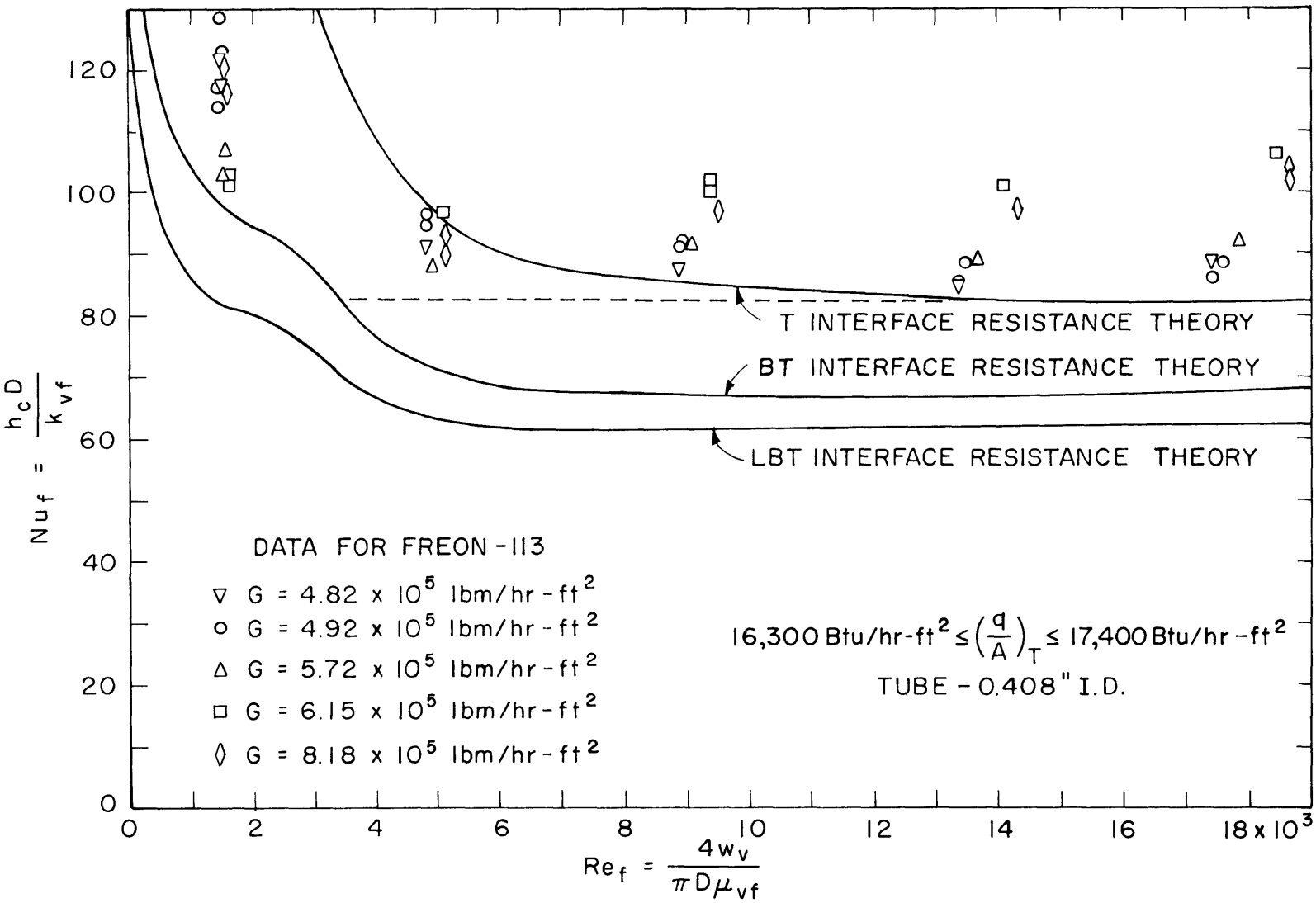

FIG. 14 EFFECT OF LIQUID VELOCITY FOR CONSTANT HEAT FLUX

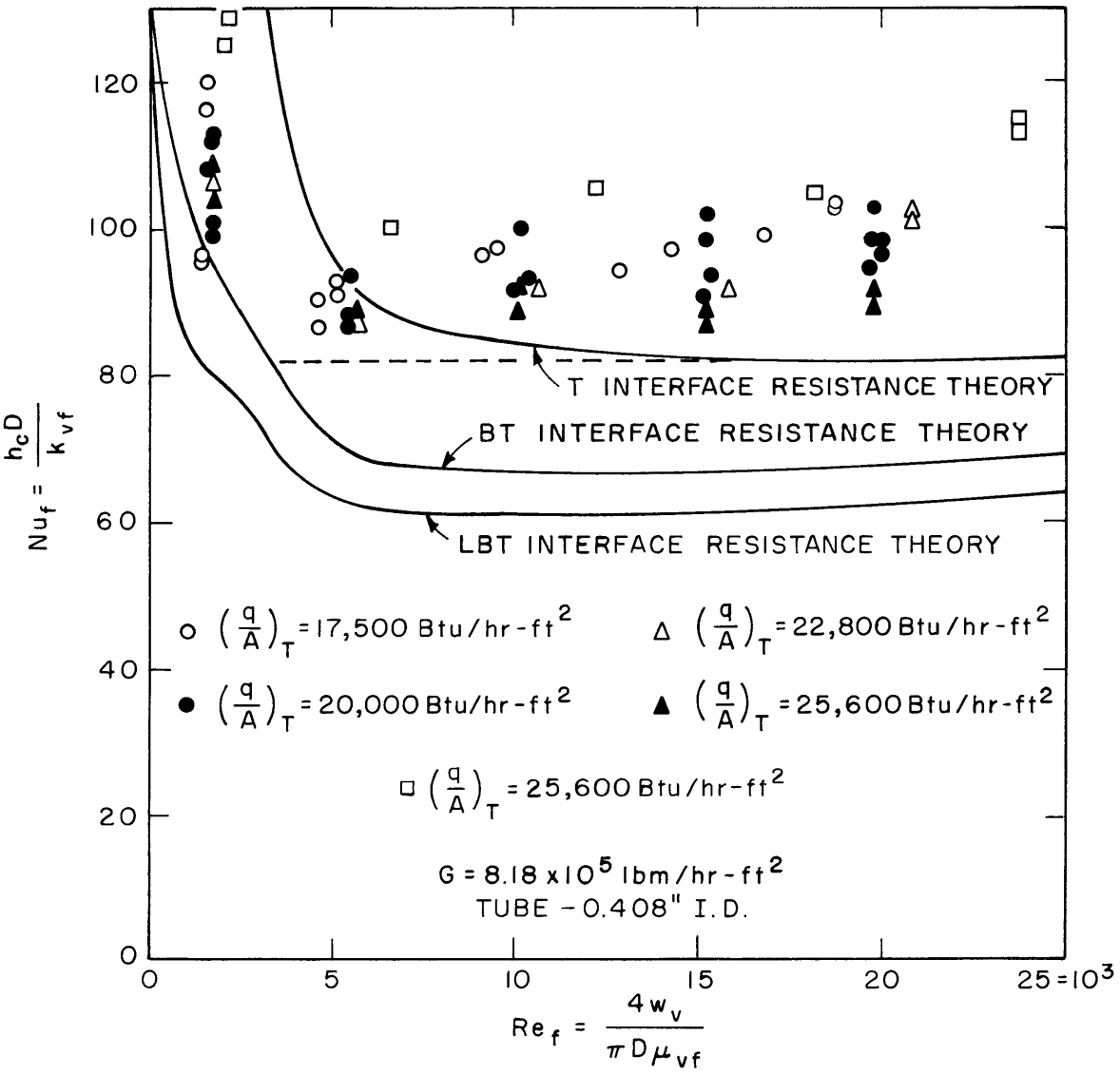

FIG. 15 EFFECT OF HEAT FLUX FOR CONSTANT MASS VELOCITY

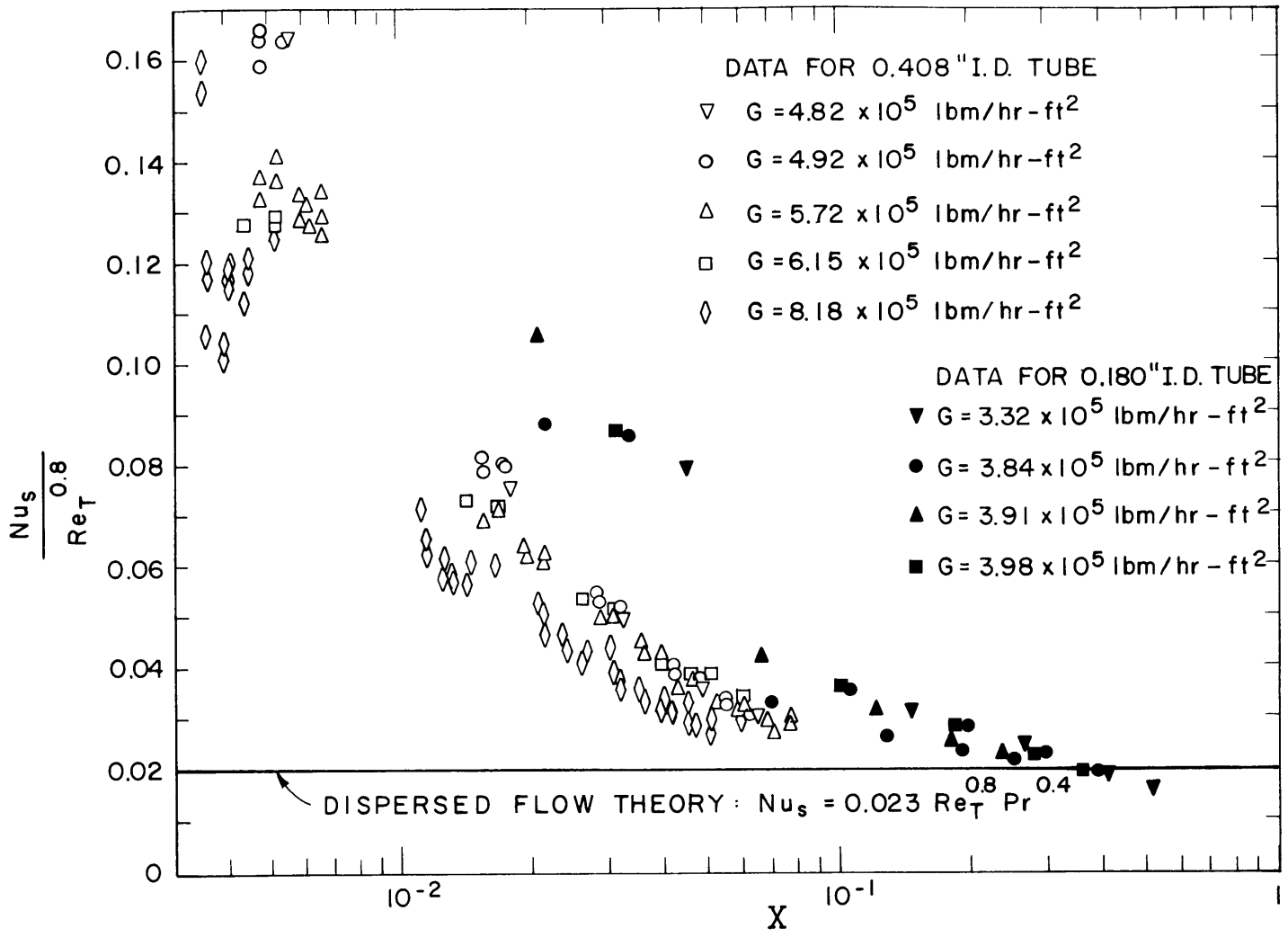

FIG. 16 APPROACH OF THE DATA TO THE DISPERSED FLOW THEORY WITH INCREASING QUALITY

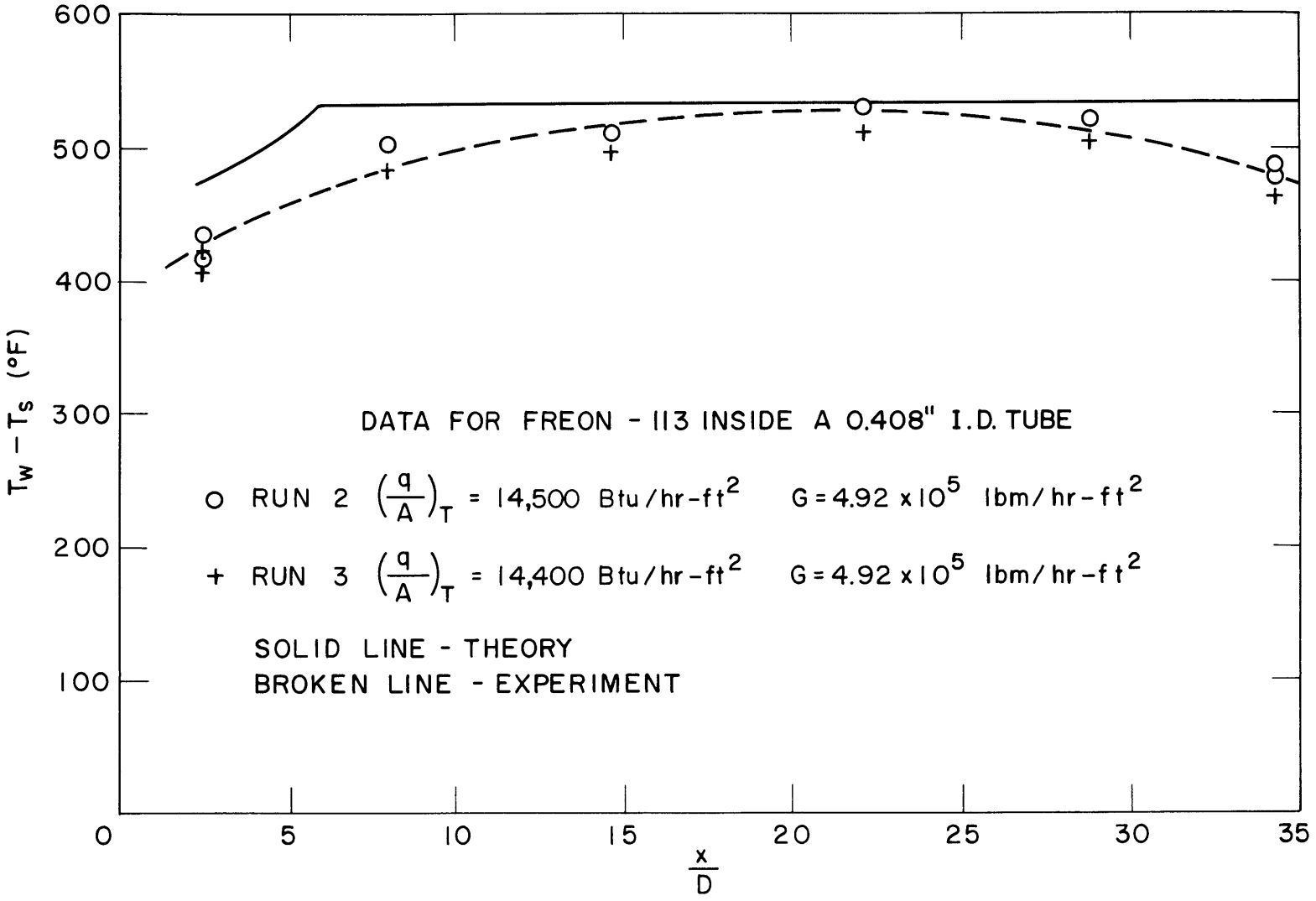

FIG. 17 TEMPERATURE DISTRIBUTION ALONG 0.408" I.D. TUBE FOR $\left(\frac{q}{A}\right)_T$ = 14,500 Btu/hr – ft^2

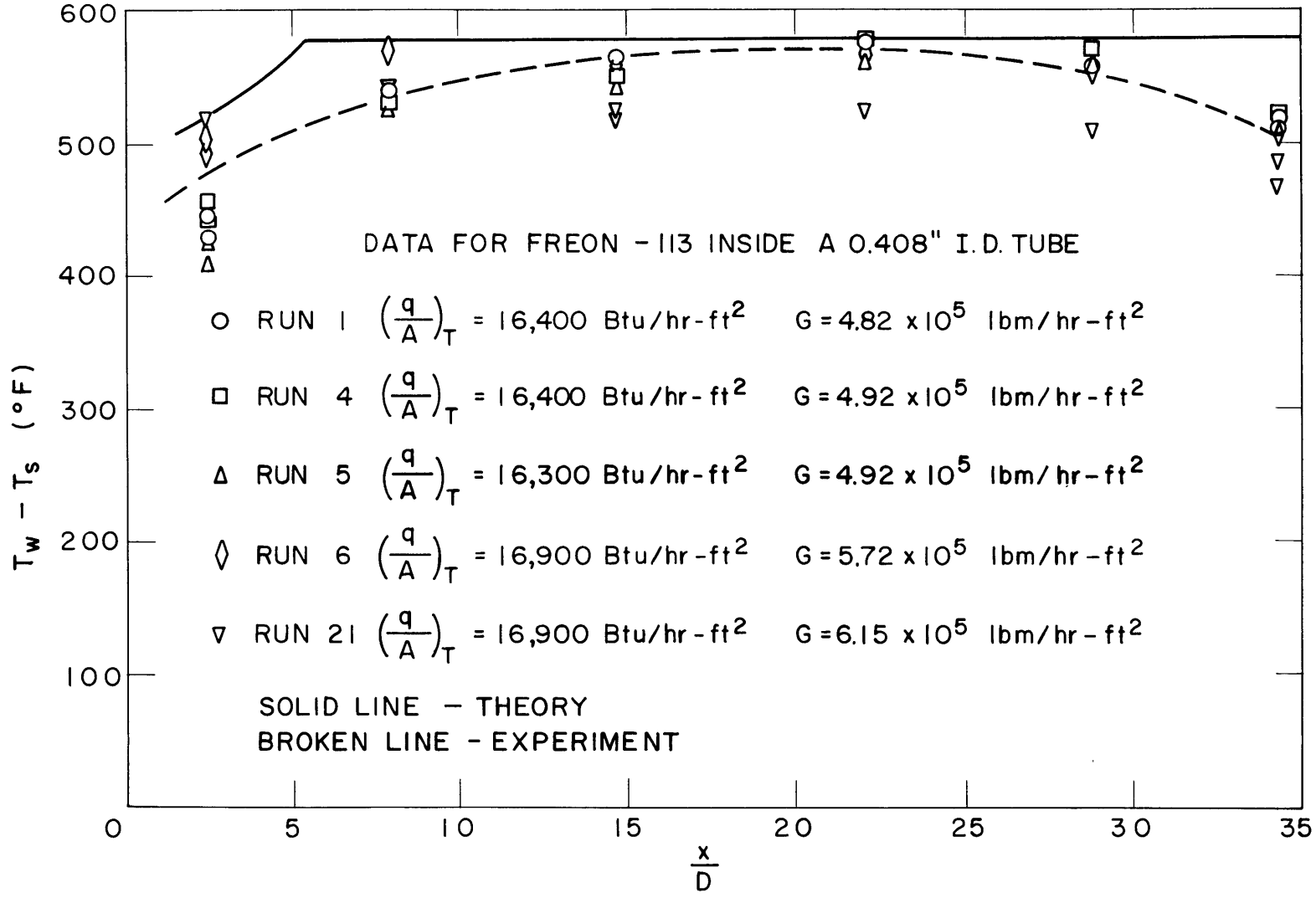

FIG. 18 TEMPERATURE DISTRIBUTION ALONG 0.408" I.D. TUBE FOR $\left(\frac{q}{A}\right)_T$ = 16,600 Btu/hr - ft^2

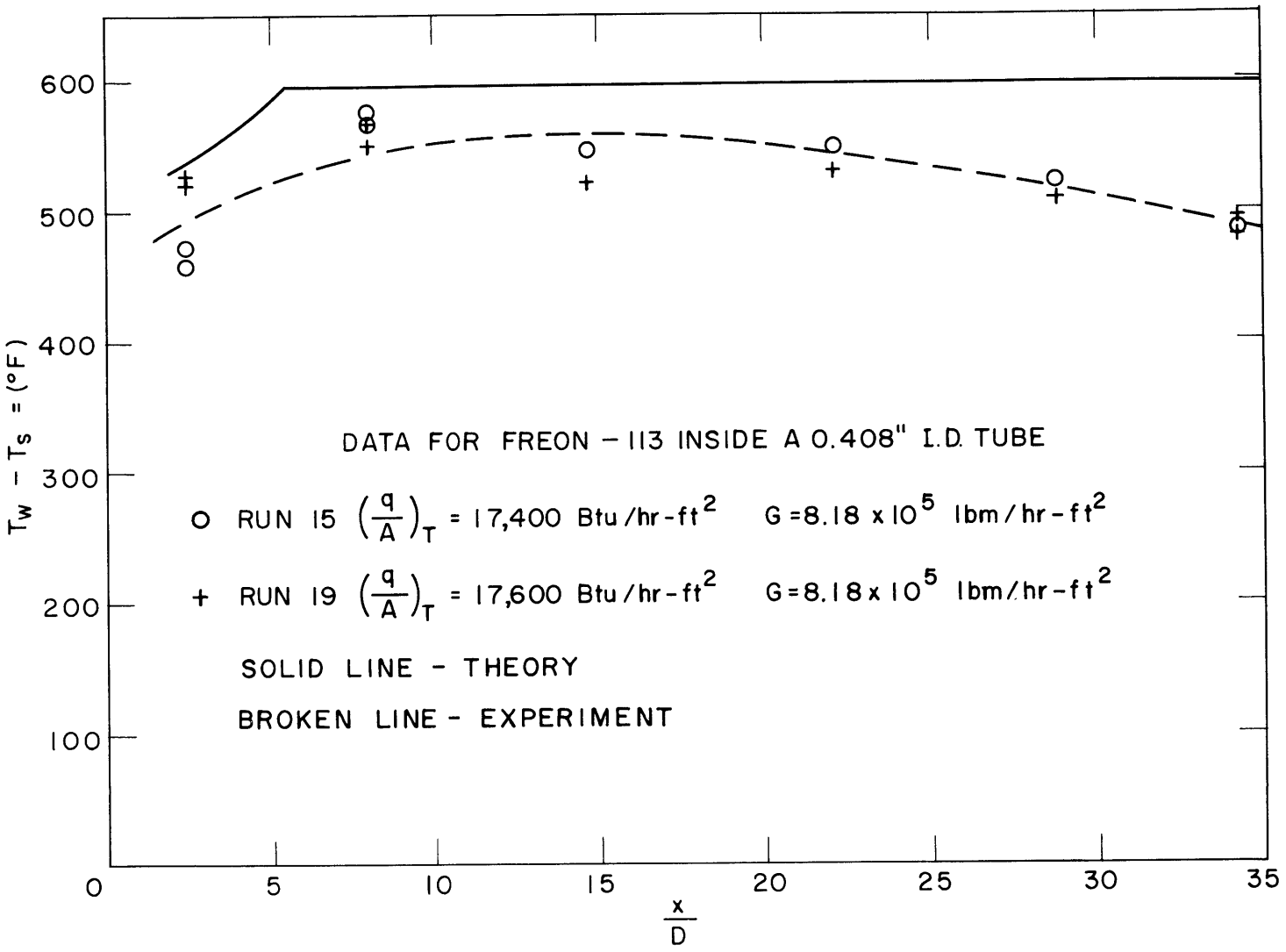

FIG. 19 TEMPERATURE DISTRIBUTION ALONG 0.408" I.D. TUBE FOR $\left(\frac{q}{A}\right)_T$ = 17,500 Btu/hr – ft^2

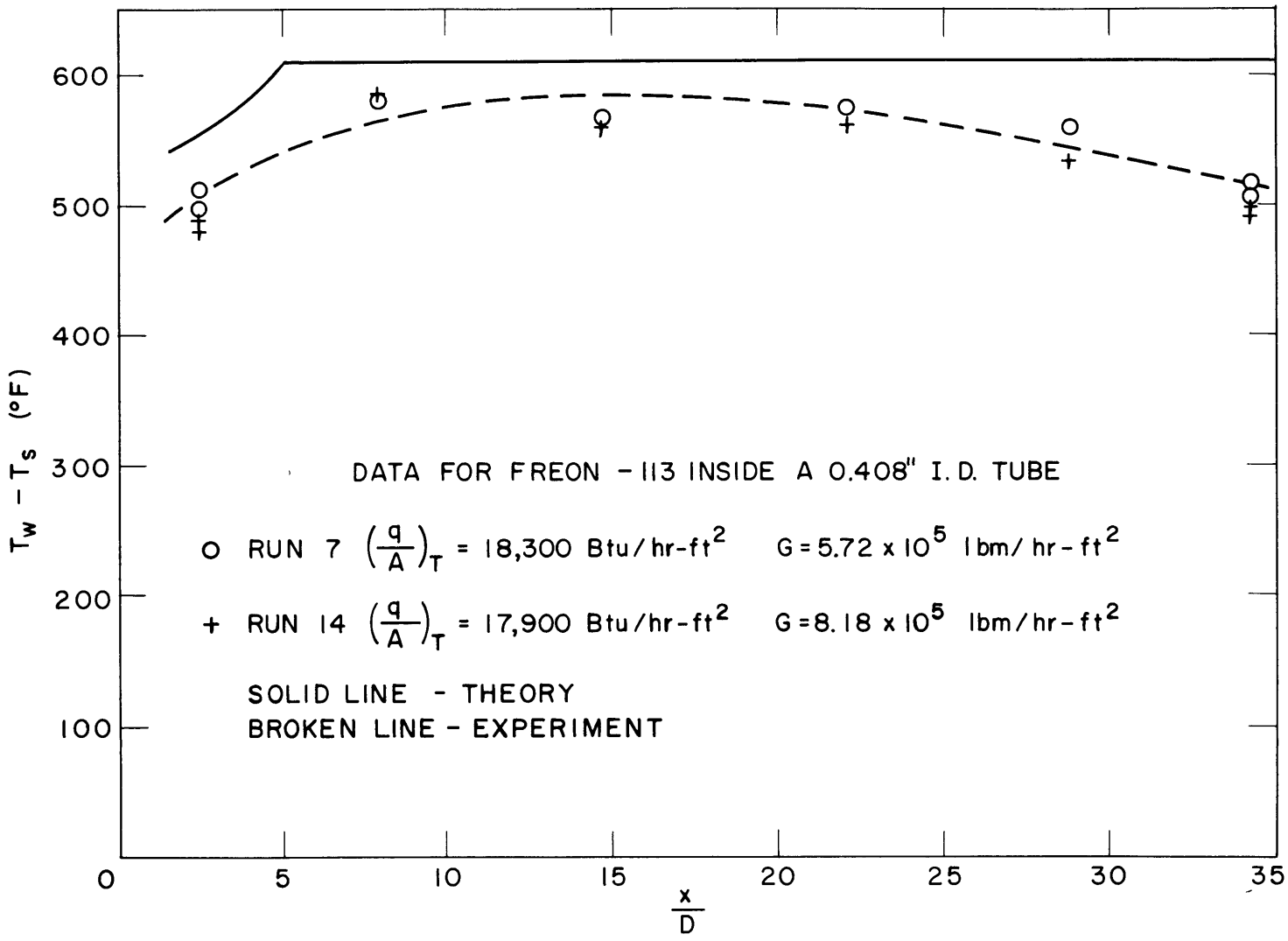

FIG. 20 TEMPERATURE DISTRIBUTION ALONG 0.408" I.D. TUBE FOR $\left(\frac{q}{A}\right)_T$ = 18,100 Btu/hr - ft^2

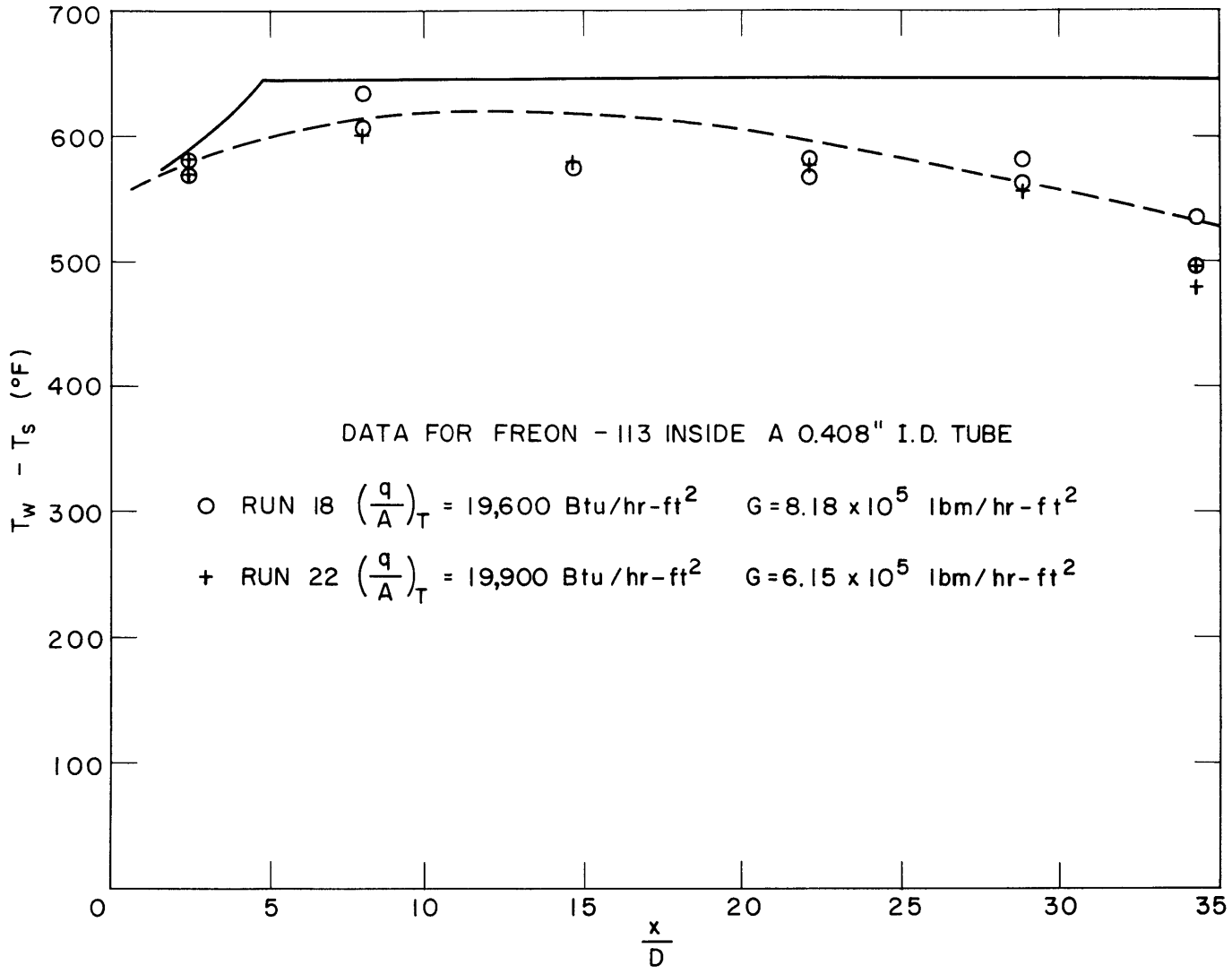

FIG. 21 TEMPERATURE DISTRIBUTION ALONG 0.408" I.D. TUBE FOR $\left(\frac{q}{A}\right)_T$ = 19,800 Btu/hr-ft^2

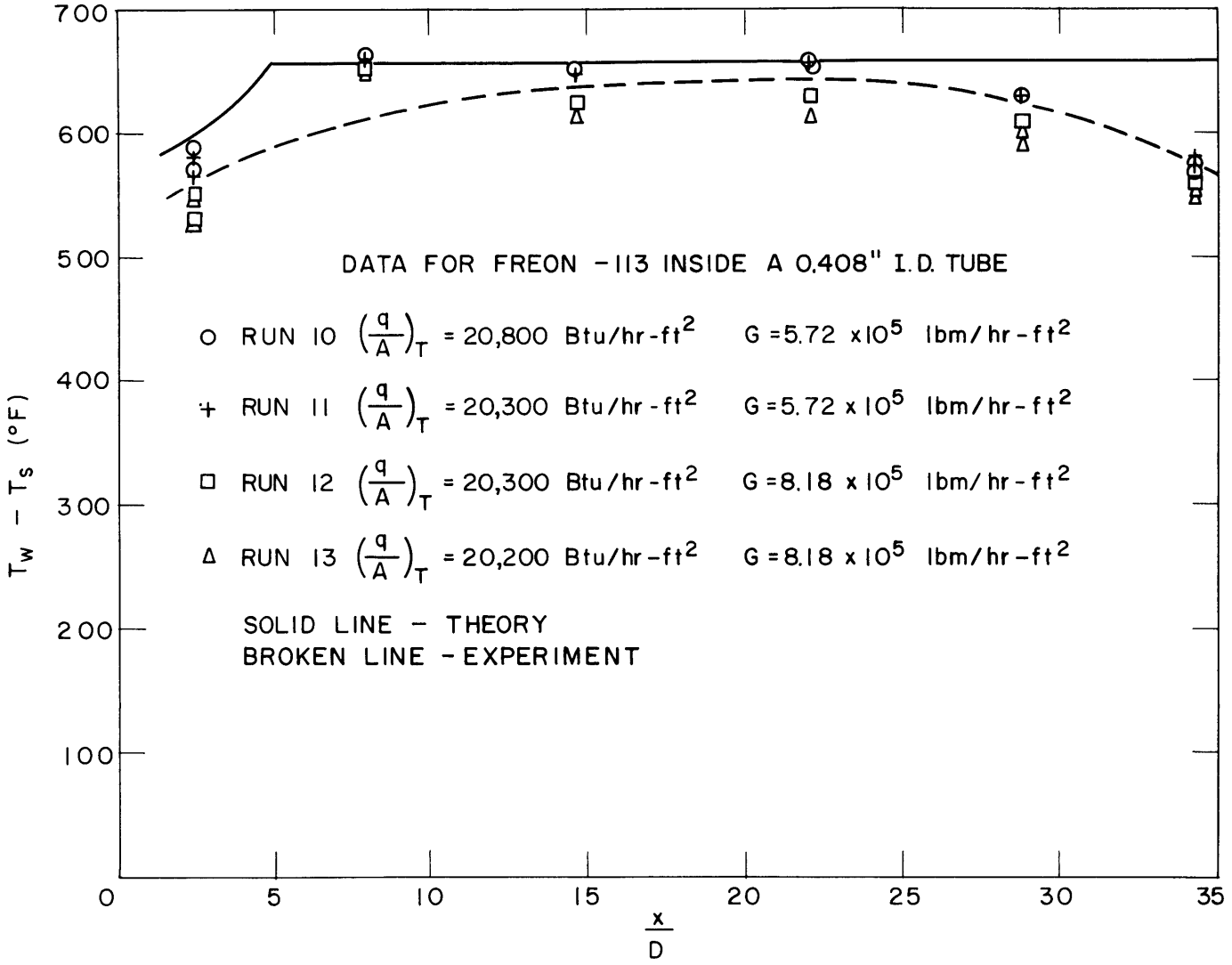

FIG. 22 TEMPERATURE DISTRIBUTION ALONG 0.408" I.D. TUBE FOR $\left(\frac{q}{A}\right)_T$ = 20,400 Btu/hr - ft^2

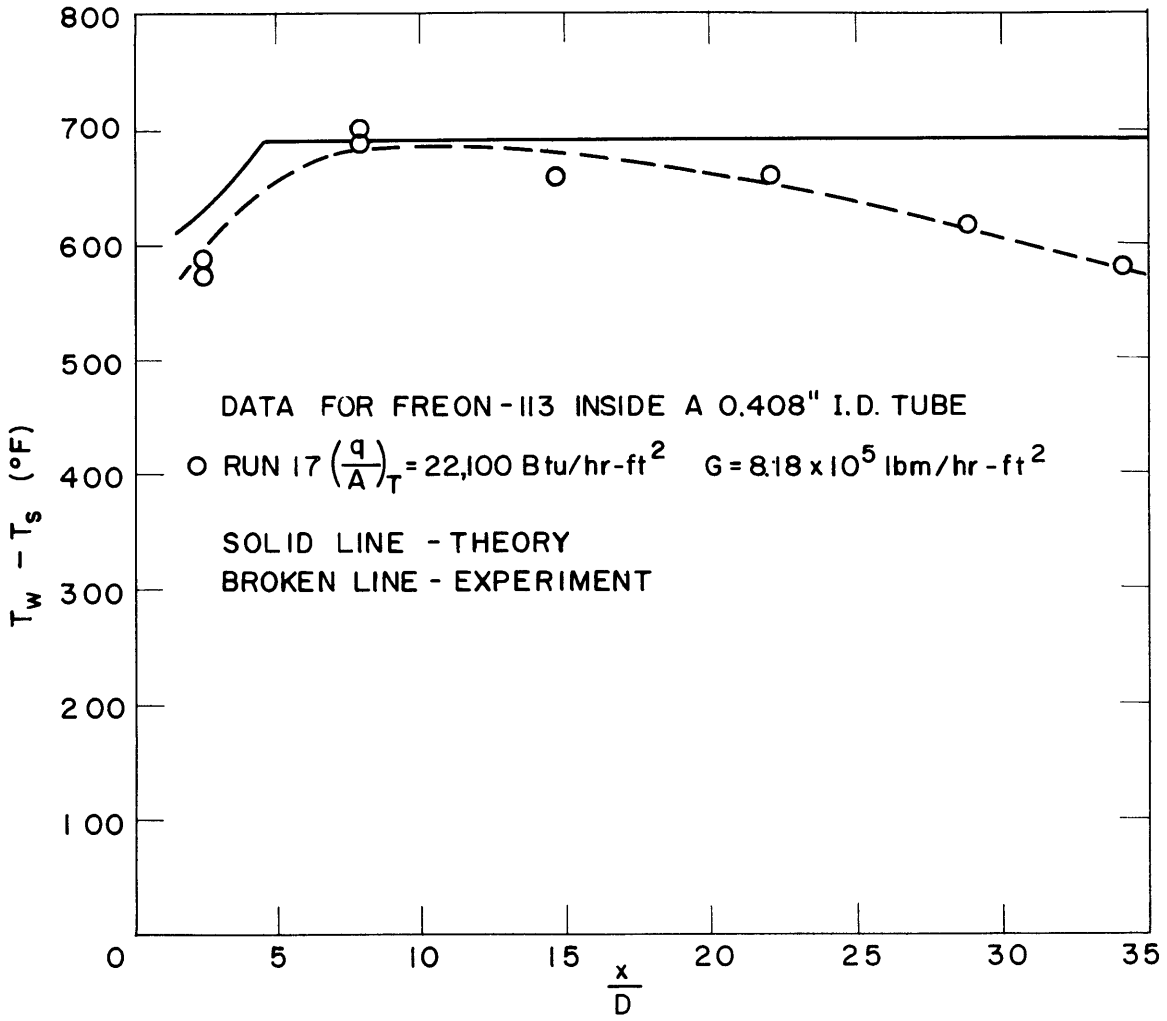

FIG. 23 TEMPERATURE DISTRIBUTION ALONG 0.408" I.D. TUBE FOR $\left(\frac{q}{A}\right)_T$ = 22,100 Btu/hr-ft^2

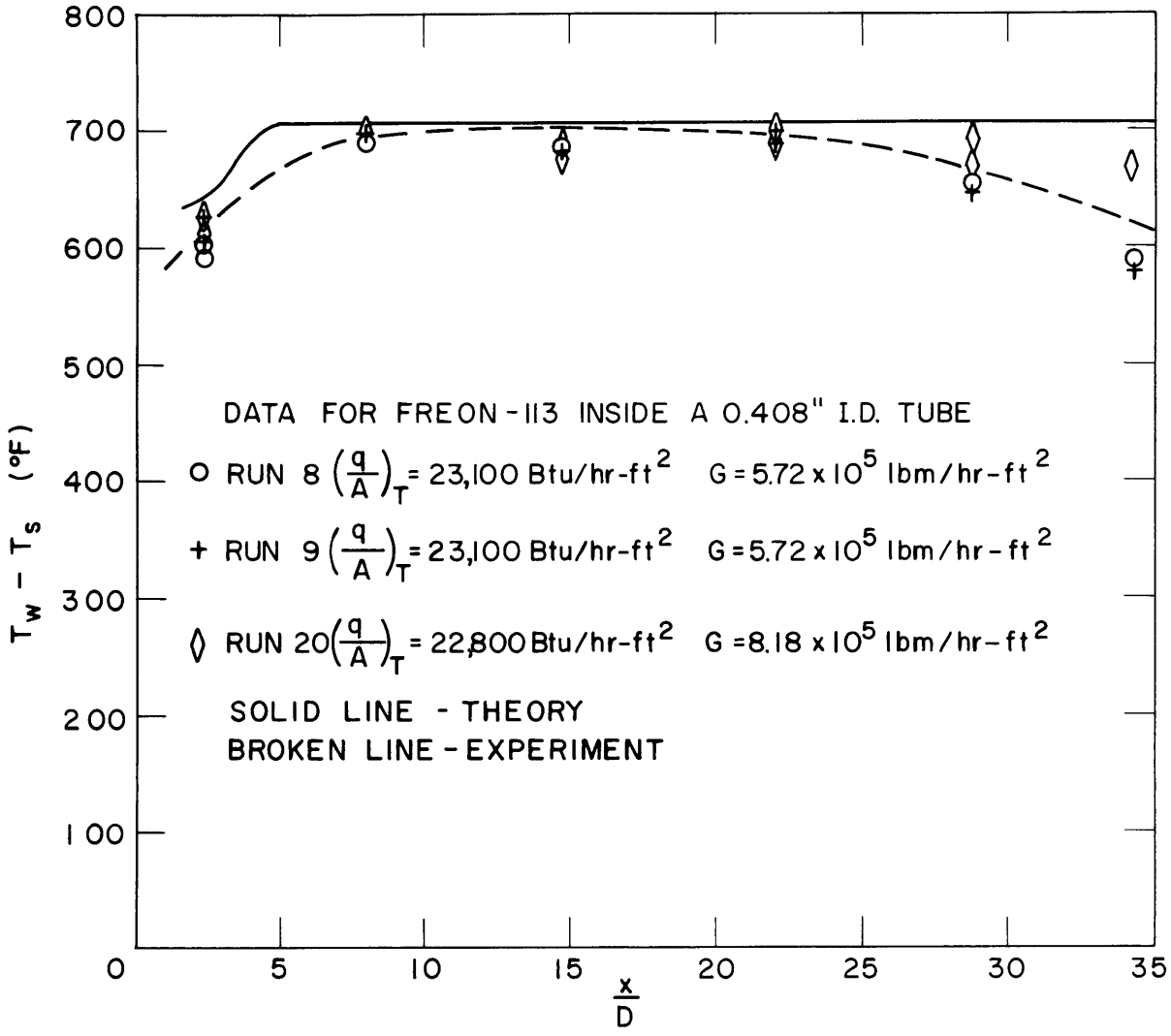

FIG. 24 TEMPERATURE DISTRIBUTION ALONG 0.408" I.D. TUBE FOR $\left(\frac{q}{A}\right)_T$ = 23,000 Btu/hr-ft^2

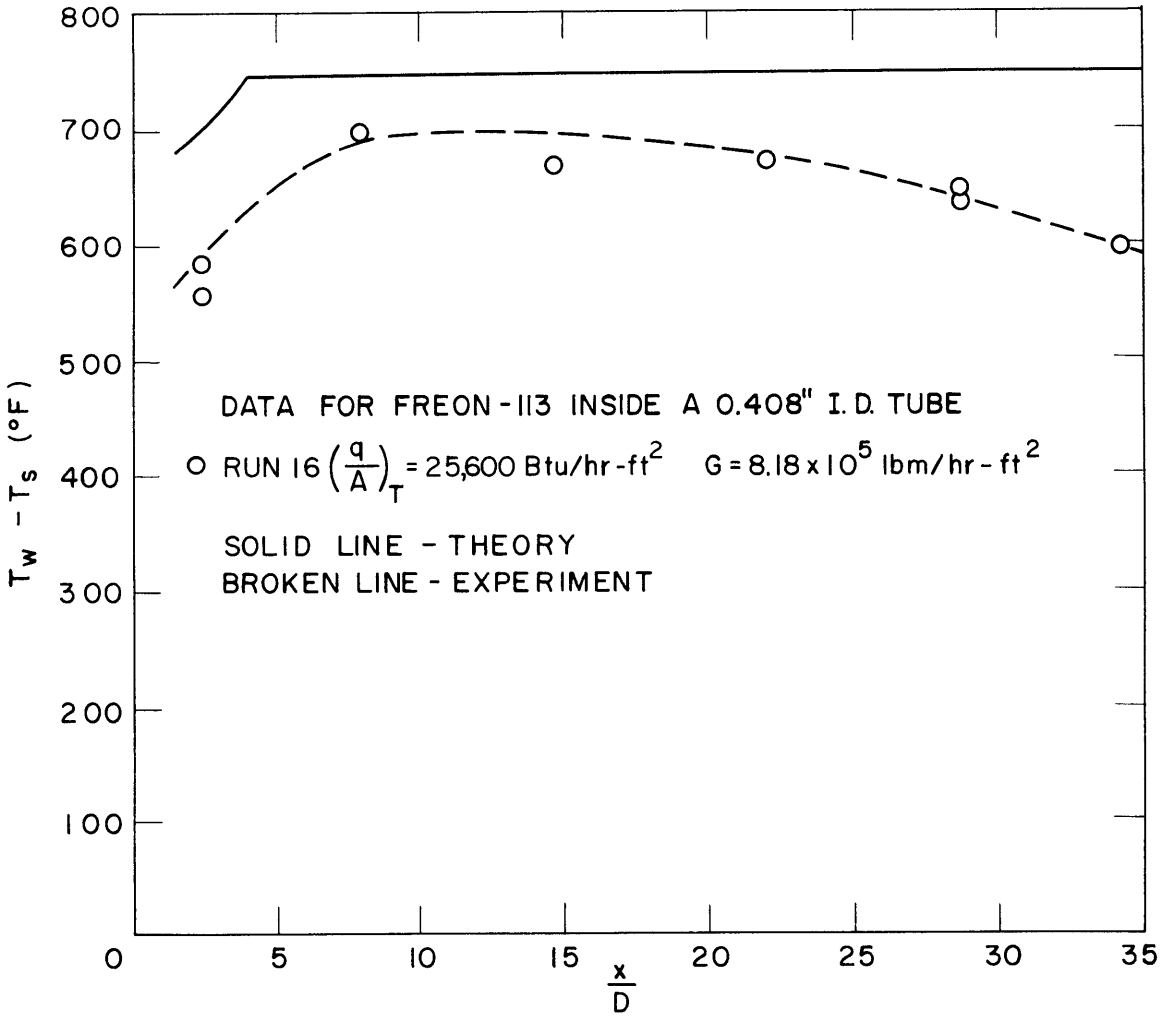

FIG. 25 TEMPERATURE DISTRIBUTION ALONG 0.408" I.D. TUBE FOR $\left(\frac{q}{A}\right)_T$ = 25,600 Btu/hr-ft^2

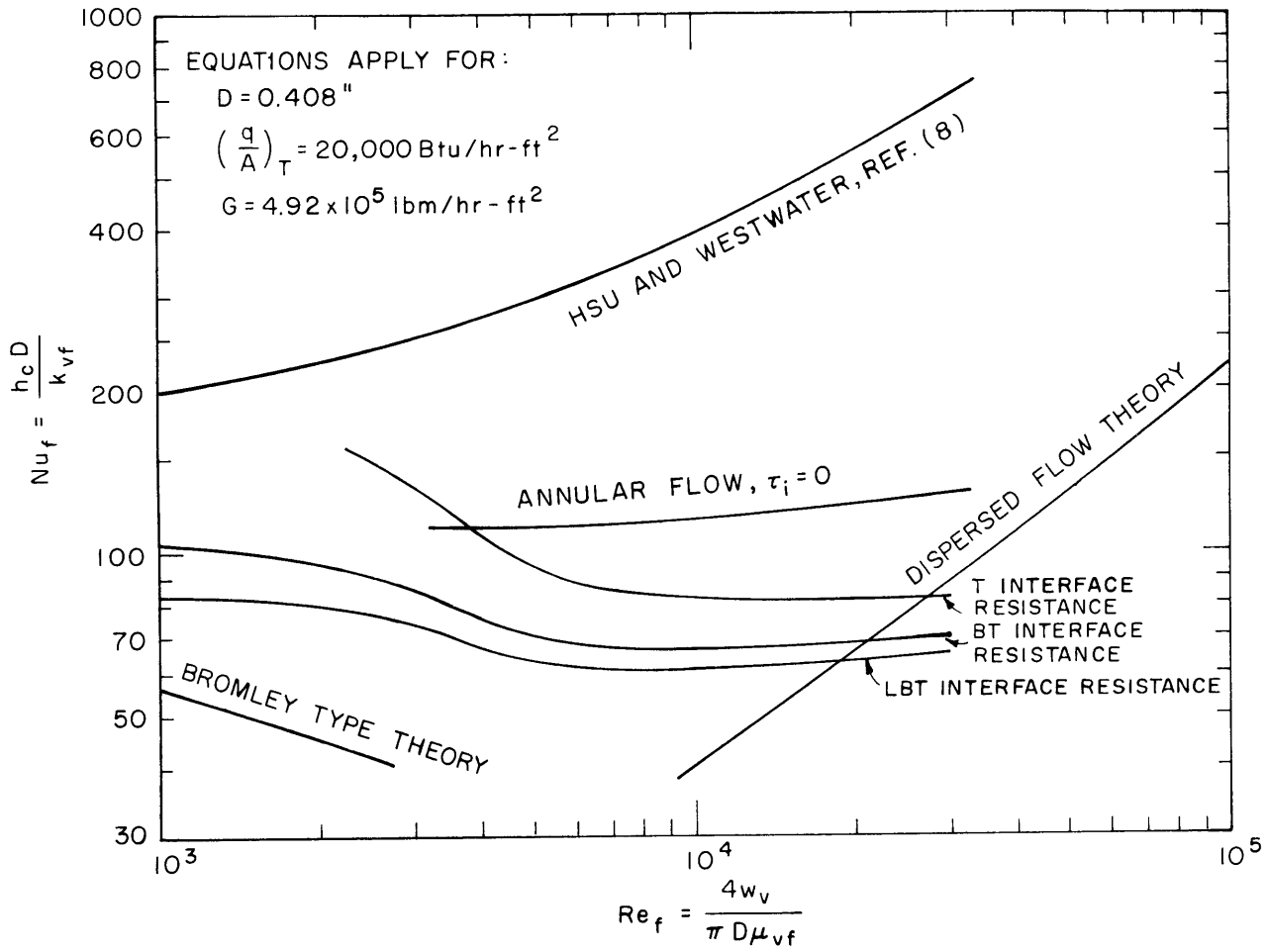

FIG. 26 COMPARISON BETWEEN VARIOUS FILM BOILING THEORIES

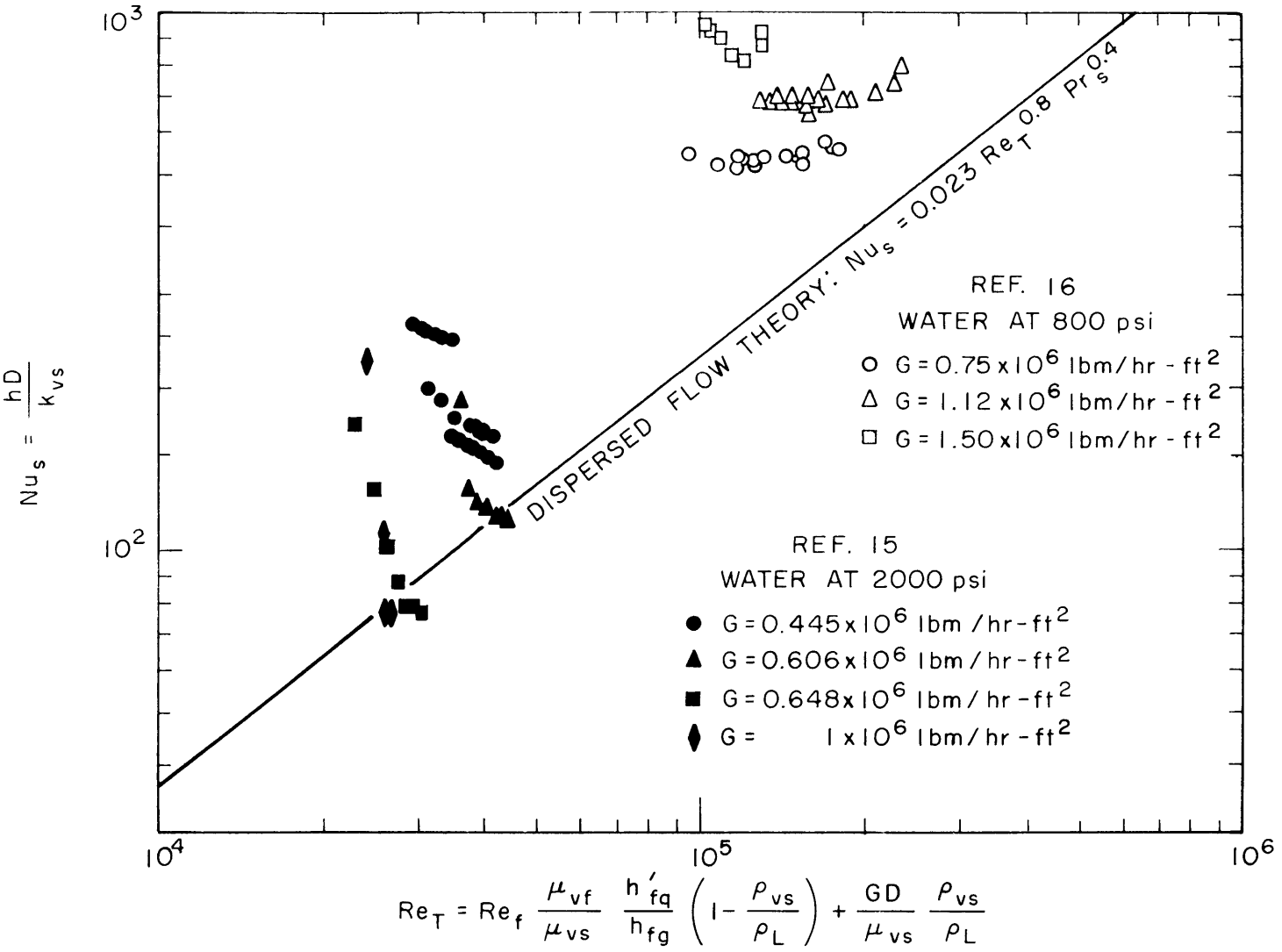

FIG. 27 COMPARISON BETWEEN DISPERSED FLOW THEORY AND AVAILABLE DATA FOR WATER

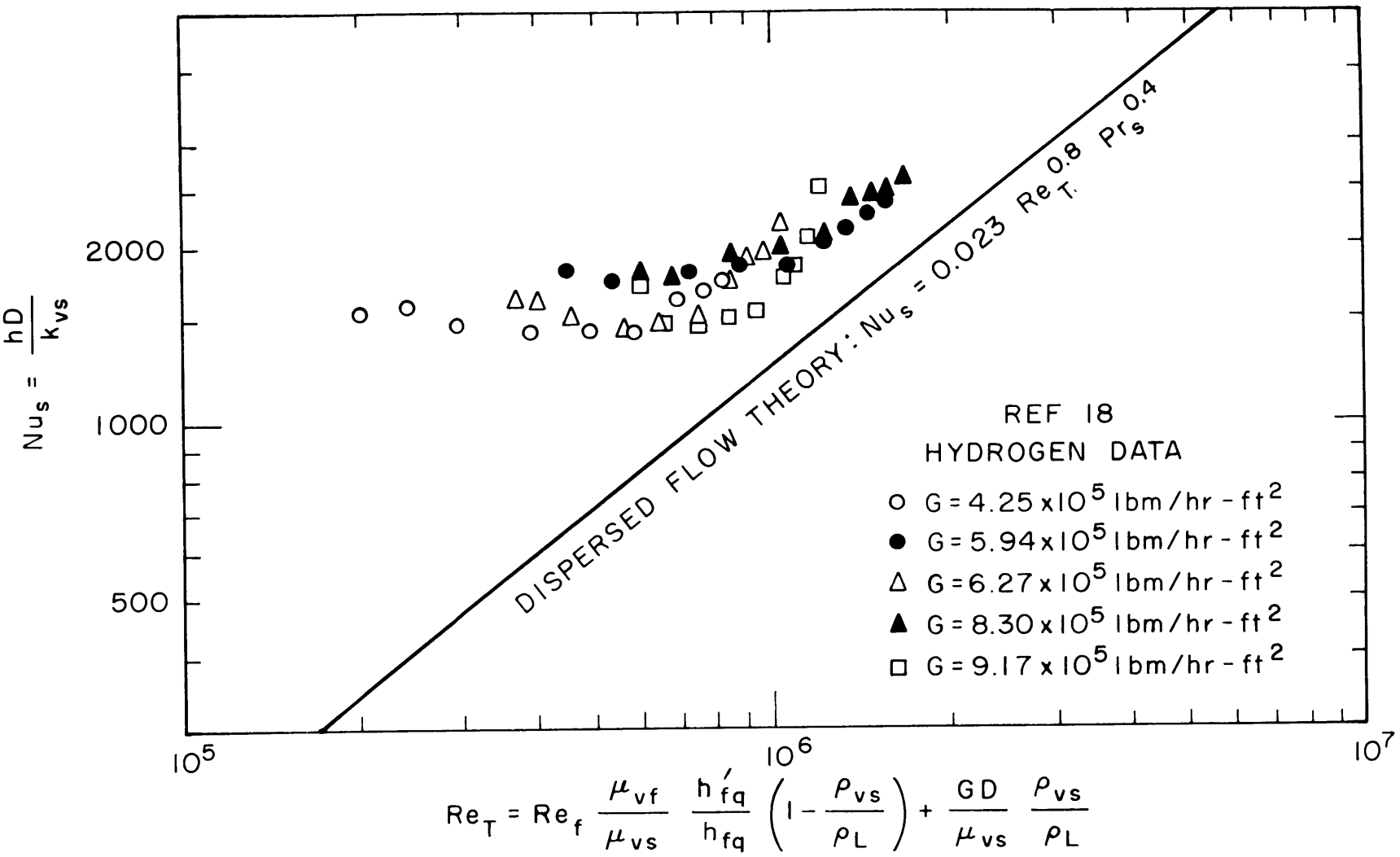

FIG. 28 COMPARISON BETWEEN DISPERSED FLOW THEORY AND AVAILABLE DATA FOR LIQUID HYDROGEN